DEGREE PROJECT IN ELECTRICAL ENGINEERING,
SECOND CYCLE, 30 CREDITS
STOCKHOLM, SWEDEN 2016

Voltage Stability Assessment of Power Systems by Decision Tree Classification and Preventive Control by Pre-Computing Secure Operating Conditions

V S NARASIMHAM ARAVA

KTH ROYAL INSTITUTE OF TECHNOLOGY
SCHOOL OF ELECTRICAL ENGINEERING

VOLTAGE STABILITY ASSESSMENT OF POWER SYSTEMS BY DECISION TREE CLASSIFICATION AND PREVENTIVE CONTROL BY PRE-COMPUTING SECURE OPERATING CONDITIONS

by

V S Narasimham Arava

A thesis submitted in partial
fulfillment of the requirements for the
degree of

Master of Science in Electric Power Engineering

KTH Royal Institute of Technology

October 2016

Supervisor: Jan Lavenius

Supervisor & Examiner: Luigi Vanfretti

**Electric Power and Energy Systems Department,
KTH Royal Institute of Technology,
Sweden**

ABSTRACT

This thesis presents a method that performs voltage stability assessment and suggests fast remedial actions against voltage instability by using decision trees and pre-calculated optimal power flow solutions.

Typically, two types of incidents cause voltage instability. The first type of incident is associated with the demand not being met due to limited transmission or reactive power reserves. The second type of incident is a major event affecting the generation or transmission system in such a way that the pre-event demand cannot be satisfied with the available generation or transmission capacity. The time left to take remedial action for the second type of incident is relatively shorter than the first type. Sufficiently fast detection and appropriate remedial actions can prevent the system from undergoing a voltage collapse. These considerations motivate the development of methods to identify operating conditions that are near or within the region for which the system is voltage unstable, and to suggest remedial actions to bring back the system to a condition where it has sufficient margin to voltage collapse.

The main contributions of the thesis are the classification of operating conditions using decision trees for voltage security assessment and the use of pre-calculated optimal power flow solutions for remedial actions. Case studies were performed on IEEE 9-bus system for several operating conditions and different network configurations. In the case studies, the time taken to retrieve the pre-calculated OPF solution was found to be considerably smaller than the time taken to compute the OPF solution online. The average load shedding was observed to be higher for the pre-calculated OPF solutions compared to the OPF solutions calculated online. The shorter time the proposed method takes to identify voltage instability, and to provide remedial actions, could be a useful tool for the power system operator to steer away the system from unstable conditions during the critical time just after being subjected to a contingency.

SAMMANFATTNING

Detta examensarbete presenterar en metod för att bedöma spänningsstabilitet och föreslå avhjälpande återgärder mot instabilitet genom att utnyttja beslutsträd och färdigberäknade lösningar av den optimala lastfördelningen.

I allmänhet är det två typer av händelser som kan orsaka spänningsinstabilitet. Den första typen är associerad med att efterfrågan inte kan mötas på grund av begränsningar i överföringskapacitet eller i tillgänglig reaktiv effekt. Den andra typen är stora störningar som påverkar kraftgenereringen eller överföringskapaciteteten så att efterfrågan, på den nivå som den låg innan störningen, inte kan tillgodoses med den tillgängliga kapaciteten i överföring eller kraftgenerering. Den tillgängliga tiden för att ta avhjälpa problemet för den andra typen av händelser är kortare än den första. För att kunna hindra spänningskollaps måste detektion och avhjälpning av instabilitet ske tillräckligt fort. Detta är en anledning till att utveckla metoder som kan identifiera situationer i kraftsystemet då detta är nära eller i regionen där systemet är spänningsinstabilt och vidare föreslå avhjälpande åtgärder som styr systemet till ett tillstånd då det har en tillräckligt stor marginal till spänningskollaps.

De huvudsakliga bidragen i detta examensarbete är klassificeringen av driftstillståndet genom beslutsträd för att bedöma spänningsstabilitet samt användningen av färdigberäknade lösningar av den optimala lastfördelningen för att föreslå avhjälpande åtgärder. Fallstudier utfördes på ett kraftsystem med nio noder, IEEE 9-bus system, med en uppsättning av olika konfigurationer av ledningssystemet. I fallstudierna visade det sig att den föreslagna metoden var avsevärt snabbare jämfört med att beräkna den optimala lastfördelningen vid den aktuella tidpunkten. Den förkortade tid det tar att identifiera instabilitet och föreslå åtgärder kan vara ett användbart verktyg för systemoperatörer då de ska styra systemet från en instabil driftsituation under den kritiska tid som uppstår alldeles efter system har blivit utsatt för en oväntad störning.

TABLE OF CONTENTS

LIST OF FIGURES

LIST OF TABLES

ACKNOWLEDGMENTS

Foremost, I would like to express my sincerest gratitude to Luigi Vanfretti, who supported me throughout my master's with his knowledge and patience, whilst allowing me to work in my own way. I attribute my power system modeling knowledge to his teaching as part of power system research project courses. He showed me different ways to approach a research problem and the need to be persistent to accomplish any goal.

I would also like to thank Jan Lavenius, who supervised me with his insights of Power System modeling and Machine Learning. He was always there to meet and talk about my ideas, to proofread my thesis and asked me good questions to help me think through the problems (whether mathematical, computational or philosophical). I especially cherish the discussions with him about his mathematical perception of power system problems.

Last, but not least, I thank my family for their unconditional support and encouragement to pursue my interests, even when the interest went beyond the boundaries of field and geography.

ACRONYMS

ANNs. Artificial Neural Networks.

AP. Active Power

DTs. Decision Trees.

HVDC. High Voltage Direct Current.

LTC. Load Tap Changer.

OPF. Optimal Power Flow.

PMU. Phasor Measurement Unit.

RP. Reactive Power

SNB. Saddle Node Bifurcation.

VSI. Voltage Stability Index.

VCPI. Voltage Collapse Proximity Indicator.

Chapter I

1. INTRODUCTION

1.1 Background

Voltage stability refers to the ability of a power system to maintain steady voltages at all buses in the system after being subjected to a disturbance from a given initial operating condition[1]. Voltage drops or voltage losses occur when electric power is transferred through a transmission network between the generation and load points. In normal operating conditions, these voltage drops are within the acceptable limits of the grid [2]. But due to disturbances, increases in power consumption, or other system changes can cause the bus voltages to vary significantly from their acceptable operating range (which are set by power system operators or grid code) in such a way that operator intervention or automatic control fails to halt this deviation. During these circumstances, voltages may experience large, progressive falls, which are so pronounced that the system integrity is endangered and power cannot be delivered to the loads. This is referred to as voltage instability and its result is termed as voltage collapse. These voltage-related threats to system security are expected to become more severe over the next decades as the demand for electric power is increasing [3]. The change in energy portfolio and ecological concerns restrict the construction of new transmission lines and makes it impossible to construct new non-renewable generation plants.

Voltage instability phenomena time frame ranges from seconds to hours and studies were done with appropriate models [2]. Table 1.1 lists some historical voltage instability incidents [3].

Table 1.1 Examples of historical voltage instability incidents

Date	*Location*	*Time Frame*
13/04/1986	Winnipeg, Canada Nelson River HVDC link	Short term, 1 sec
30/08/1986	SE Brazil, Paraguay-Itaipu HVDC link	Short term, 1 sec

17/05/1985	South Florida, USA	Short term, 4 sec
27/12/1983	Sweden	Long term, 55 sec
30/12/1982	South Florida, USA	Long term, 1-3 min
04/08/1982	Belgium	Long term, 4-5 min
22/09/1977	Jacksonville, Florida	Long term, few min

All these events caused interruptions in the power supply to consumers and resulted in losses of billions of dollars [3]. Online voltage stability monitoring is an effort towards an early detection and mitigation of such voltage instability events.

Voltage instability usually occurs in power systems that are heavily loaded or faulted or has shortage of reactive power. Typically, two types of incidents causes voltage instability problem. The first type of incident is associated with the demand not being met with the available transmission or reactive power reserves. This situation may result from unexpected large load increase and/or an earlier weakening of the system, such as low voltages and increased losses. The second type of incident is a major event affecting the generation or transmission system in such a way that the demand, which is the pre-fault consumption, cannot be satisfied with the available generation or transmission capacity.

Voltage Stability Indices (VSI) were developed to deal with the first type of incidents. These indices help to foresee unacceptable effects of load increments. Moreover, this anticipation capability along with inherent delay in some cases of load increments (because of the type of loads) gives the operator some time to take remedial actions like switching capacitor banks, changing the generator voltage set points, etc. However, the picture is quite different for voltage instabilities that can follow major incidents such as outage of a large capacity generator that is producing its maximum rated power or the disconnection of heavily loaded transmission lines. The time left to take remedial action for the second incident is relatively shorter than the first type of incident. This short time is very important and early detection of a critical state can prevent the system from collapsing.

These above considerations motivate the development of approaches that can help in early identification of voltage instability and suggest remedial actions to bring back the system to stable state. Machine learning techniques like Decision Trees (DTs) can offer useful tools to handle the early identification of voltage instability and suggest remedial actions.

1.2 Problem Definition

Machine learning techniques like DTs, clustering algorithms, neural networks and statistical methods are widely applied for on-line voltage stability assessment. These methods can create/use a model, which is based on knowledge of the operator decisions or historical data. In this thesis, decision trees is being used for voltage stability assessment and to suggest preventive actions that can be given as an input to system operators or automatic load shedding schemes. The decision tree is a white-box model that can be applied when the functioning/working of a system is unknown or very complex, but there is plenty of data available. These models do not explicitly model the physical system, but establish a mathematical relationship between a large numbers of input-output pairs measured from the system. The mathematical relationship is a model of the system, which can be computed numerically from the measurements or simulated outputs. The accuracy of the model may vary depending on the how accurate the simulated outputs replicates the behavior of original system.

The idea of this approach is to enlarge and generalize the existing security boundary method of "stable" and "unstable" region to classify the operating regions based on distance from the nearest Saddle-Node Bifurcation (SNB) point, which is further explained in chapter 2.

1.3 Objectives

The objective of this thesis is to develop a method that is applicable in practice and which that makes use of the data from a power system model for voltage security assessment and for calculating curative actions. In more detail, the sub-tasks to be solved in this thesis are,

- Formulate and simulate an optimization problem which maximizes the distance to the nearest saddle node bifurcation point.
- Create a database with power flow outputs of several operating points for different network configurations and use them to train the decision trees.
- Testing the decision trees with respect to random time domain simulation outputs (voltage magnitude, active power consumption at load buses).

The main focus of the thesis is to use DTs for voltage security assessment and then use pre-calculated optimal power flow (OPF) solutions to take curative action for the given power system model data. In order to achieve good results from the trained DTs, the system should be modelled accurately in the power system analysis software for several different operating points and power system configurations. A large number of power system operation points and voltage stability margins must be computed in order to have DTs with good classification accuracy, which is explained in detail in chapter 2.

1.4 Overview of the report

The thesis is divided into five chapters:

Chapter 1: INTRODUCTION This chapter gives a brief introduction to voltage stability, methods used to identify voltage stability problems and short description about the context of the thesis work along with objectives and contributions.

Chapter 2: THEORETICAL BACKGROUND This chapter provides theoretical background for the voltage stability problem and methods used for voltage stability analysis in power systems. This chapter further also introduces basic concepts of Decision Trees (DTs) and Optimal Power Flow (OPF).

Chapter 3: PROPOSED VOLTAGE STABILITY INDEX This chapter explains the methodology used for voltage stability assessment using indices with an illustrative example.

Chapter 3: A METHOD FOR VOLTAGE STABILITY ASSESSMENT USING DECISION TREES This chapter describes the methodology/work flow adopted in the thesis to create and use decision trees for voltage stability assessment in power systems.

Chapter 5: A METHOD FOR LOOKING UP PRE-CALCULATED PREVENTIVE ACTIONS AGAINST VOLTAGE PROBLEMS This chapter describes the formulation of OPF method based on maximization of the distance to voltage collapse and the methodology/work flow used to implement this method in the thesis.

Chapter 6: CASE STUDIES This chapter presents the results and observations based on the results obtained by applying the proposed approach explained in previous chapters for the given network.

Chapter 7: CLOSURE This chapter provides the summary of the complete work in the thesis along with the conclusions inferred from the obtained results and future work details.

Appendix contains the data of the test bus system used for simulations in the thesis.

Chapter 2

2. THEORETICAL BACKGROUND

2.1 Voltage Stability

According to IEEE, the standard definition for voltage stability "… is the ability of the power system to maintain steady voltages at all the buses in the system after being subjected to a disturbance from a given initial operating condition. It depends on the ability to maintain/restore equilibrium between load demand and load supply from the power system [1]." Voltage instability is a non-linear phenomenon. It is impossible to capture the phenomenon as a closed-form solution [3]. The instability is manifested once the network crosses the maximum deliverable power limit.

2.1.1 Classification of voltage instability

Based on the severity, voltage instabilities can be classified into four different categories [1].

Large disturbance voltage stability refers to the system's ability to maintain steady voltages following large disturbances such as system faults, loss of generation, or circuit contingencies.

Small disturbance voltage stability refers to the system's ability to maintain steady voltages when subjected to small perturbations such as incremental changes in system load.

Short term voltage stability involves dynamics of fast acting load components such as induction motors, electronically controlled loads and HVDC converters. The study period of interest is in the order of several seconds and analysis requires a solution of appropriate system differential equations.

Long term voltage stability involves slow acting equipment such as tap-changing transformer, thermostatically controlled loads and generator current limiters. The study period of interest may extent to several or many minutes

and long-term simulations are required for analysis of system dynamic performance.

2.1.2 Methods to assess voltage stability

In this section, voltage stability assessment by some common analysis methods is briefly explained.

2.1.2.1 PV curves

PV curves or "nose curves" can be used to illustrate the basic phenomena associated with voltage instability [4]. These curves are obtained by plotting the active power transfer *P* across a grid interface versus the voltage magnitude *V* at a bus of interest. With increase in load, the voltage at the load bus decreases and reaches a critical value that corresponds to maximum power transfer. In general this maximum power transfer is related to voltage instability if the load is constant power type. Beyond this point there is no equilibrium. Knowing this point can determine the stability margin of the grid for a certain operating point in a certain direction. However, if the load type is other than constant power then the system can operate below the critical voltage, but draws higher current for the same amount of power transfer.

Consider the a simple two bus system as shown in figure 2.1 with an infinite bus V_1 connected to a load that consumes the complex power $\overline{S}_L = P_L + jQ_L$, through a loss-less transmission line with reactance X.

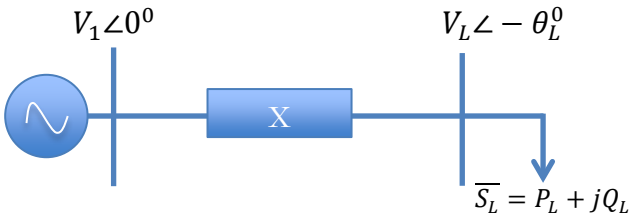

Figure 2.1 A simple two bus system

Active Power (AP) consumption at the load bus is given by,

$$P_L = \frac{V_1 V_L}{X}\sin(\theta_L) \tag{2.1}$$

Reactive Power (RP) consumption at the load bus is given by,

$$Q_L = -\left(\frac{V_L^2}{X} - \frac{V_1 V_L \cos(\theta_L)}{X}\right) \tag{2.2}$$

The voltage angle $\theta_L$can be eliminated by using the relation $sin^2\theta + cos^2\theta = 1$, which can result in the following equation.

$$(V_L^2)^2 + (2Q_L X - V_1^2)V_L^2 + X^2(P_L^2 + Q_L^2) = 0 \tag{2.3}$$

Since (2.3) is a quadratic equation, solving for V_L^2gives the following expression

$$V_L = \sqrt{\frac{-(2Q_L X - V_1^2) \pm \sqrt{(2Q_L X - V_1^2)^2 - 4X^2(P_L^2 + Q_L^2)}}{2}} \tag{2.4}$$

But $Q_L = P_L tan\varphi$, where $\cos(\varphi)$ is the load power factor, and assumed to be constant. Substituting $Q_L = P_L tan\varphi$ in (2.4) gives the following.

$$V_L = \sqrt{\frac{-(2P_L X tan\varphi - V_1^2) \pm \sqrt{(2P_L X tan\varphi - V_1^2)^2 - 4X^2 P_L^2 (sec^2\varphi)}}{2}} \tag{2.5}$$

For different values of P_L, V_L has four solutions. Out of the four solutions of V_L only two are physically meaningful. These two physical solutions correspond to high voltage (blue colour) and low voltage (red colour) solution as shown in figure 2.2. Since the power systems are designed for high voltages and low currents, the solutions in the upper side of the curve are considered. It can be observed from the figure that the two solutions coalesce at a point called the critical point or saddle-node bifurcation point or the point of maximum power transfer. The maximum power is termed as the theoretical transfer limit and the voltage is termed as critical voltage. This point indicates the maximum power that can be transferred to that load bus before power system becomes unstable.

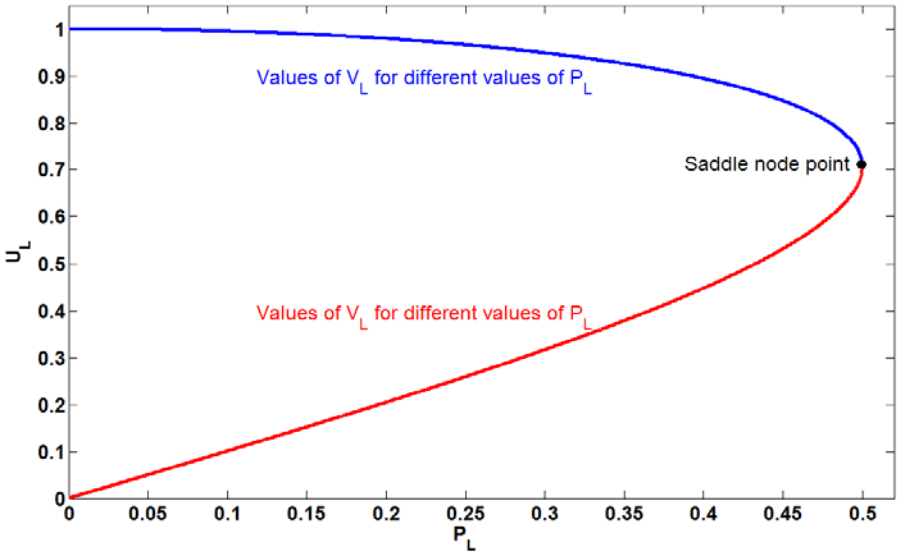

Figure 2.2 P-V curve

Figure 2.3 shows a family of PV curves for different power factors.

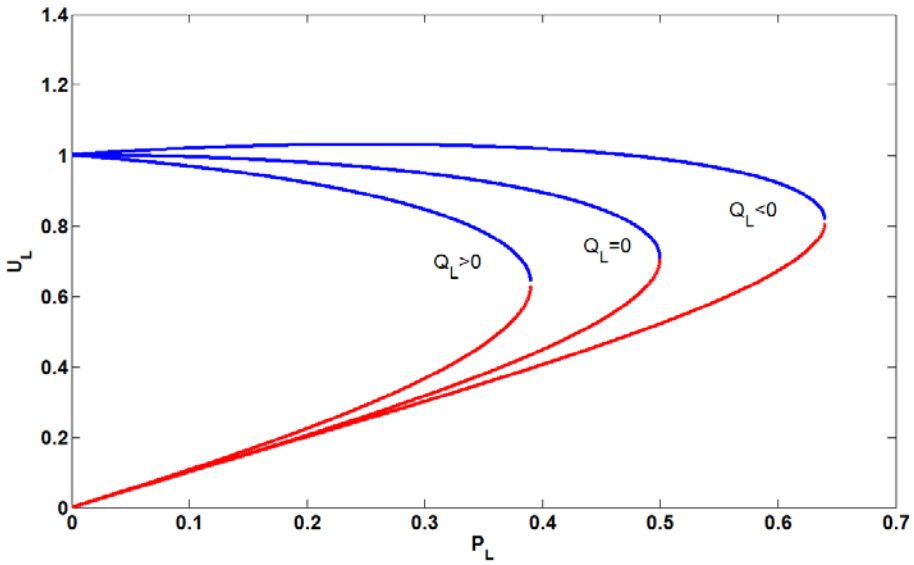

Figure 2.3 P-V curves with different power factors

The PV curve for the load shows the dependency of the power consumed by the load with respect to the bus voltage magnitude. This curve depends on the load characteristics [5]. The commonly referred PV curve is the network PV curve. It is the network voltage dependency due to changes in the load consumption at a particular bus. There are a number of factors such as the generator reactive power limit, contingencies, load dynamics etc., that affect

the distance between the nose point and the current operating point. By understanding these factors the system can be moved away from the saddle node point and make it stable.

2.1.2.2 QV curves

PV curves can be used to understand how the active power transfer affects the load bus voltage. But in order to understand the impact of reactive power transfer, the concept of QV curves is important. For the given bus of interest, these curves can be used to illustrate the reactive power requirement at a given bus to maintain certain voltage for a fixed value of active power transfer. A QV curve can be determined by connecting a fictitious generator with $Pg = 0$ and unlimited reactive power capacity to a PQ bus as shown in figure 2.4.

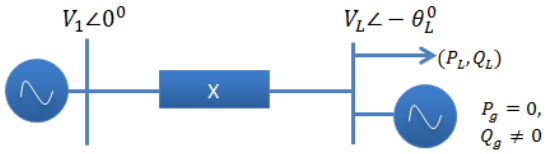

Figure 2.4 Connection of a fictitious generator to calculate the QV curves

The QV curves are determined by successive power flow calculations [3]. The reactive power generated versus the voltage at the fictitious generator gives a plot such as the one shown in figure 2.5. It should be noted that $Qg < 0$ indicates the generator absorbs/consumes reactive power and $Qg > 0$ indicates that the generator injects/produces reactive power.

The intersection between the QV curve and $Qg = 0$ gives the operating point/solution of the system. For the cases when the QV curve intersects $Qg = 0$ then the system is stable in the region where the gradient of the Q-V curve is positive i.e. the voltage level will increase if the reactive power is injected. The critical operating point is reached when $\frac{dQ_g}{dU_L} = 0$. The voltage at this point is the critical voltage as shown in figure 2.5. Hence, power system is stable on the right hand side of the minimum and unstable to the left hand side [4]. If the QV curve does not intersect $Qg = 0$, then there is no

operating point in the system i.e. the system is unstable. These simulated curves can be used to evaluate the reactive power compensation at the bus of interest. Figure 2.5 shows two Q-V curves representing two different transfers of AP.

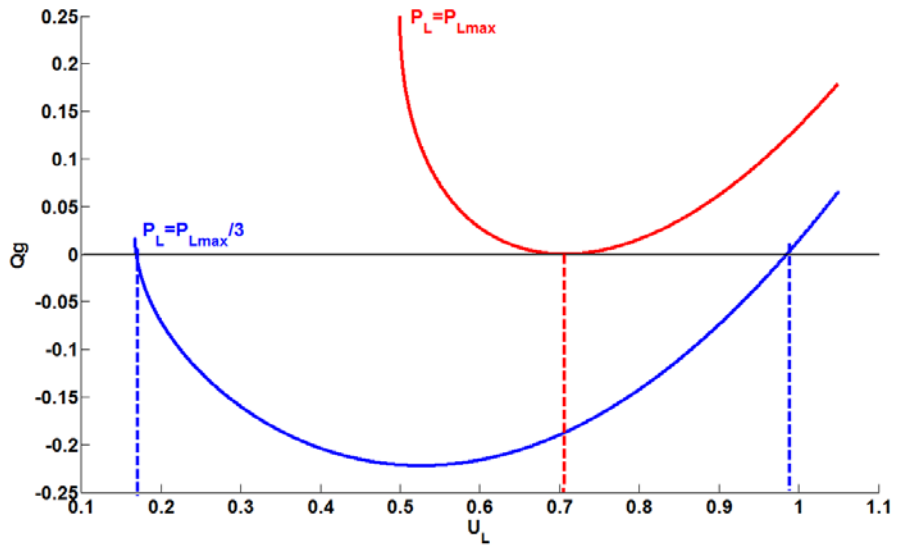

Figure 2.5 Q-V curve with different active power loading

The intersection between the Q-V curve and the dashed line corresponds to no compensation. The reactive power compensation required to maintain a specific voltage at the load bus can be obtained from figure 2.5.

2.1.2.3 Q-V sensitivity

One way to identify the buses in the grid that are prone to voltage collapse is to calculate the Q-V sensitivity at the selected buses [6]. The Q-V sensitivity represents the slope of the $\frac{\Delta Q}{\Delta V}$ curve at the selected bus at a given operating point. A criterion for voltage stability is that at a given operating point for every bus "*i*"

$$\frac{dQ_i}{dV_i} > 0 \tag{2.6}$$

where Qi is the injected reactive power at bus "*i*". The physical interpretation of (2.6) is that reactive power at a bus "*i*" will result in increasing of the

voltage magnitude of bus "*i*". The system is voltage unstable if for any bus "*i*", the condition (2.6) is not satisfied [3].

A positive slope represents stable operation, i.e. the bus voltage increases when the reactive power injection is increased. The smaller the gradient of the positive slope, the less sensitive the system will be. As the sensitivity index increases towards infinite value when the loading is increased, the system approaches a state of instability. Therefore, the weaker buses can be identified by determining which have the steepest positive slopes.

2.1.2.4 Voltage Collapse Proximity Indicator (VCPI)

VCPI is another way to identify the weak buses in the system [3, 7]. The index varies from close to unity during lightly loaded conditions to infinity at a collapse situation. The VCPI can be used to determine the most effective locations for emergency load shedding or reactive power compensation.

$VCPI_Q$ relates how the total generation of reactive power in the system is affected by an increase in reactive power load at bus "*i*". The VCPI with respect to reactive power is given by,

$$VCPI_{Q_i} = \frac{\sum_{j \in G_k} \Delta Q_{gj}}{\Delta Q_i}, i \in G_L \tag{2.7}$$

Where G_k is the set of the generator buses and G_L is the set of studied load buses. ΔQ_i represents a small increase in reactive power demand at the studied bus "*i*" and ΔQ_{gj} is the change in reactive power output at generator "*j*" for change in reactive power demand at the studied bus "*i*". The weakest bus of the studied grid is determined by identifying the bus with the highest $VCPI_Q$ value. Bus "*m*" will thus be the weakest bus of the current operating point of the given system if the (2.8) holds.

$$VCPI_{Q_m} = \max\{VCPI_{Q_i}\}, i \in G_L \tag{2.8}$$

2.1.3 Voltage instability mechanisms

In this section, some grid mechanisms that could lead the system into a state of voltage instability are discussed. These mechanisms are not usually

instability mechanisms by themselves, but in a heavily loaded power system they trigger the voltage instability phenomena.

2.1.3.1 Load Tap Changing (LTC) transformers

An LTC is a transformer with variable turns-ratio. LTC transformers are commonly used in power transmission systems to add an additional level of control. The function of LTC is to control the voltage at the load by changing the turns-ratio. The taps are located on the high voltage side of the transformer because the current rating is less on high voltage side when compared to low voltage side, which prevents the sparking when there is tap changing in the transformer. Moreover, high voltage winding is easy to access because it is wound over the low voltage winding. So, because of these reasons the taps are located on the high voltage side of the transformer providing control of low voltage side. The voltage control capability of the LTC transformers plays an important role in load restoration following a disturbance in the grid.

Consider a fictitious power system which is fully loaded. Due to a disturbance, one of the transmission lines is disconnected that further increases the loading on other available transmission lines. Outage of the fully loaded transmission line will cause a voltage drop at the nearby load centers. This further increases the power demand of the system due to increased current consumption by the loads. To counteract this voltage drop, the LTC transformers in the area will attempt to restore the voltage in the distribution grid (which is set based on the grid code/operator). Each change in tap ratio to restore load bus voltage further increases the stress on the system because the increase in load voltage leads to increase in load power consumption (since it is voltage dependent). An increase in load power implies higher current through the transmission system that results in higher losses. These additional losses will further decrease the voltage level of the transmission system. But LTC function is based on the local voltage, it still tries to maintain the voltage at the load bus. This increases the load power consumption that leads to increased current consumption. This further leads

to increase in losses in the system. To compensate the demand in the system, the connected generators increase their generation. Eventually, generators would hit the current limits governed by over-excitation limiters and cause its terminal voltage to drop. This causes the difference between increased demand and generation eventually leading to a voltage collapse situation.

The driving force behind the voltage collapse situation is the load restoration performed by LTC transformers. A run-down situation causing voltage instability occurs when the load dynamics attempt to restore power consumption beyond the capability of the transmission network and the connected generation to provide the required reactive power support.

2.1.3.2 Stalling of Induction motors

Induction motors are most commonly used electric motors in industry due to its low maintenance and robustness. Induction motors is one of the reasons for fast voltage instability due to its fast load-restoring actions. After a disturbance such as tripping of a long transmission line or short circuit, Induction motor responds quickly to match the mechanical torque as shown in (2.9)

$$2H\dot{s} = T_m - T_e(U_L, s) \tag{2.9}$$

where H is the inertia constant, T_m is the mechanical torque, T_e is the electrical torque, s is the motor slip and $U_L$is the voltage at the bus where motor is located. Torque is the twisting force that causes the rotation and Slip of an induction motor is the difference between the synchronous speed and induction motor speed at full load. Further details can be found in [8]. Due to increased impedance, the motor mechanical and electrical torque curves may not intersect after the disturbance, leaving the system without post-disturbance equilibrium point. As a result the motor stall and the network voltage collapse.

2.1.4 Prevention of voltage instability

In [9]-[10], a number of different preventive and corrective actions to counteract voltage instability are comprehensively described. However, we

limit our discussion to two different corrective actions to prevent voltage instability.

Reactive power support should take place close to the load which leads to decrease of power losses in the transmission system, and an increase of the maximum deliverable active power to the loads. This can be performed by switching on the shunt capacitor banks, switching off shunt inductors in the transmission system, synchronous condensers etc.

Load reduction can be done by blocking the LTC tap changing or reducing the LTC set point or by load shedding.

2.2 Decision Trees (DTs)

With the introduction of wide area monitoring [11] in a power system, there is an abundance of data. Given the accuracy and speed of measurements, DTs are useful for applications like state estimation, feedback control systems, adaptive relaying and security monitoring. During an event or fault, this data can also be used for understanding the behavior of the system, updating parameters of the power system model and prediction of instability in the system. In this section, voltage stability assessment using DTs is explained in detail. This approach is suitable for online applications because the time consuming calculations are done offline and therefore the decision results can be obtained instantaneously.

The extraction of implicit, previously unknown and potentially useful information from data is known as "Data Mining" [12]. Although, modern power systems has a high volume of data, the need for data mining applications in power systems can be traced quite far back after the Northeast (USA) blackout in 1965. The first attempt to apply statistical pattern recognition to power system security was done by Dy Liacco in 1967 to introduce the concept of "preventive (normal)", "emergency" and "restoration" operating states [13]. The "preventive" state is the normal state wherein the system is stable with all the components within grid operating limits. The "emergency" state arises when the system begins to lose stability

or when a power system component operating constraint is violated. The "restoration" state is when service to some customers has been lost (usually due to progression through "emergency" state).

The voltage stability assessment is a classification problem. Artificial Neural Networks (ANNs) [14] and Decision Trees (DTs) [15] are the two most commonly used classification algorithms for voltage stability assessment. The advantage of DTs over ANNs is that DTs are white box models while ANNs are black box models [14]. Knowing the attribute of splitting in a DT helps us to monitor the region associated to the attribute for stability and control functions. For example, if outage of a line is causing overloading in other line leading to instability in the system. The DTs trained on the data has the power flow of the overloading line as the node that helps the user to interpret the result.

2.2.1 Illustration of a DT

A decision tree is a data representation technique that uses a branching method to separate every possible outcome of a decision [12]. The tree consists of nodes and branches. The nodes are the points in a tree where a test is done on the attribute; branches are the outcomes of the test that lead to another node. There are three kinds of nodes: root node, internal node and leaf node. Root node is the topmost node, internal node is the node which is in-between and leaf node is the end node. The completion of the test is decided by the purity of the node. If a node attains a certain pre-defined level of class purity (i.e. having only one type of output in that node) then the node is terminated. In order to classify a new sample, the attribute values are tested against the decision tree. A path is traced from root node to the leaf node that holds the class prediction for that sample. The structure and working of decision tree can be explained by using the data given in table 2.1.

Table 2.1 Illustrative example-Weather data

Outlook	Temperature	Humidity	Windy	Play Golf
Sunny	Hot	High	False	No
Sunny	Hot	High	True	No
Overcast	Hot	High	False	Yes

Rainy	Mild	High	False	Yes
Rainy	Cool	Normal	False	Yes
Rainy	Cool	Normal	True	No
Overcast	Cool	Normal	True	Yes
Sunny	Mild	High	False	No
Sunny	Cool	Normal	False	Yes
Rainy	Mild	Normal	False	Yes
Sunny	Mild	Normal	True	Yes
Overcast	Hot	High	True	Yes
Overcast	Hot	Normal	False	Yes
Rainy	Mild	High	True	No

Figure 2.6 shows the decision tree that can be obtained for the given data.

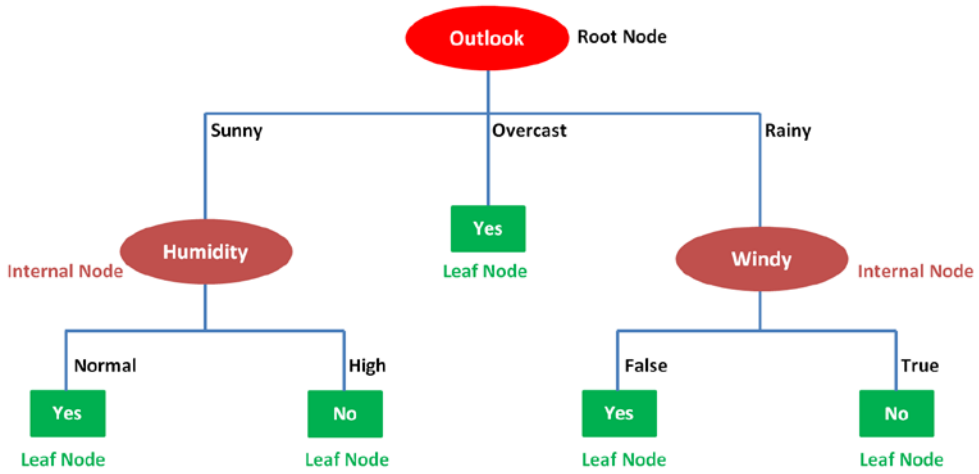

Figure 2.6 Decision Tree for the data given in table 2.1

The objective of the data in table 2.1 is to decide whether a given day is suitable for playing golf. Therefore, the class attribute 'Play Golf' needs to be predicted. The values the attribute 'Play Golf' takes are the class values. In this example there are two values to predict, i.e. 'Yes' or 'No'. All the elements in the first row are the attributes and the values they take listed along the columns are called 'Instances'.

If the attributes are continuous numbers they are called numeric attributes. As per the definitions which are defined earlier in this section, 'Outlook' is the root node, 'Humidity' and 'Windy' are the internal nodes and the decision nodes are the leaf nodes. During the construction of the decision tree, an attribute for a node is decided based on its ability to reduce the impurity (uncertainty) of the division that it produces on a dataset.

2.2.1.1 DT Building

The basic task in building a DT is to repeatedly find an attribute to be tested on a node and then branch to another node The process of finding an attribute for testing and branching is called splitting. The objective of a split in a tree is to reduce the impurity (uncertainty) in the dataset with respect to class in the next stage which can be accomplished by calculating the information gain. This calculation is done in two stages. First, the Entropy (ENT) of the dataset is measured as (2.10).

$$Entropy\ (S) = -\sum_{i=1}^{c} p_i \log_2(p_i) \tag{2.10}$$

where

c: number of classes,

S: training data/instances,

p: proportion of S classified as i.

Expected information gain is calculated by using ENT as shown in (2.11).

$$Gain(S, a) = Entropy(S) - \sum_{v \in values} \frac{|S_v|}{|S|} Entropy(S_v) \tag{2.11}$$

where

$S_v = \{s \in S: a(s) = v\}$ with v being the value of the attribute,

$Gain(S, a)$ is the expected information gain obtained from the knowledge of the attribute 'a'. Now the Entropy of the dataset in table 2.1 can be calculated as

$$Entropy(S) = -\sum_{i=1}^{c} p_i \log_2(p_i) = \frac{-9}{14}\log_2\left(\frac{9}{14}\right) - \frac{5}{14}\log_2\left(\frac{5}{14}\right) = 0.94$$

Similarly for instances of the attribute 'Outlook' the entropy values are the following:

$Entropy(S_{sunny}) = 0.97$

$Entropy(S_{overcast}) = 0$

$Entropy(S_{rainy}) = 0.97$

The expected information gains can then be calculated using (2.11),

$$Gain(S, outlook) = Entropy(S) - \sum_{v \in values(outlook)} \frac{|S_v|}{|S|} Entropy(S_v)$$

$$= 0.94 - \frac{5}{14} * 0.97 - \frac{4}{14} * 0 - \frac{5}{14} * 0.97 = 0.23$$

Similarly, expected information gain is computed for other attributes.

$Gain(S, temperature) = 0.03$

$Gain(S, humidity) = 0.15$

$Gain(S, windy) = 0.05$

It can be observed that expected information gain is highest for the attribute 'Outlook', so it is therefore chosen as the root node in figure 2.5. The attribute 'Outlook' has three instances; hence it will result in three branches. The next step is to find the attribute used for branching. Consider all the instances which have 'Outlook' to be 'Sunny'. After doing this, total number of instances in the data set decreases (reduces to 5). The entropy and expected information gain is computed for the remaining attributes.

$$Entropy(S) = -\sum_{i=1}^{c} p_i \log_2(p_i) = \frac{-2}{5}\log_2\left(\frac{2}{5}\right) - \frac{3}{5}\log_2\left(\frac{3}{5}\right) = 0.97$$

For the attribute 'Temperature' entropy for its instances,

$Entropy(S_{hot}) = 0$

$Entropy(S_{mild}) = 1$

$Entropy(S_{cool}) = 0$

The expected information gain for attribute 'Temperature' is given by,

$$Gain(S, Temp) = Entropy(S) - \sum_{v \in values(Temp)} \frac{|S_v|}{|S|} Entropy(S_v)$$

$$= 0.97 - \frac{2}{5} * 0 - \frac{2}{5} * 1 - \frac{2}{5} * 0 = 0.57$$

Similarly, expected information gain is computed for other attributes.

$Gain(S, humidity) = 0.97$

$Gain(S, windy) = 0.02$

It can be observed that the information gain is highest for the attribute 'Humidity along the branch 'Sunny'. As a result it becomes the second node. Thus, by repeating these calculations for other branches and nodes, the entire tree is developed.

2.2.2 Issues with Decisions Trees

The approach pursued in developing the above tree is called a greedy search. That is because the decision is based on what is best now and the nodes which are not included in the training are not being considered. Although this approach seems to be a good solution for the training dataset, the classifier may not do well with other datasets. This is called over-fitting [12]. Over-fitting makes the tree larger and more complex (which requires longer computation time) but do not give better the rules for the general case. A solution to this problem can be to prune the tree.

The real world applications have large amounts of data to be handled; hence scalability (ability of the system to handle the growing amount of data) becomes another prime issue. The strategy is to increase resources for computation or adaptive algorithm with better scalability features or perform data reduction. Data reduction can be achieved by data compression and/or dimensionality reduction. Data compression is the process of transforming of original data to a reduced representation. Dimensionality reduction is the process of eliminating insignificant attributes i.e. the attributes that does not give any new information for decision making.

2.3 Optimal Power Flow (OPF)

The optimal power flow (OPF) was first introduced by Carpentier in 1962 as a network-constrained economic dispatch problem [16]. The goal of OPF is to find the optimal settings of a given power system network that optimize the system objective function while satisfying the power flow equations, system security and equipment operating limits.

The objective function can be total generation cost, system loss, bus voltage deviation, emission of generating units, number of control actions and load shedding. According to the selected objective function and constraints there are different mathematical formulations for the OPF problem. They can be broadly classified as follows:

- Linear problem in which objectives and constraints are given in linear forms with continuous control variables
- Nonlinear problem where either objectives or constraints or both combined are nonlinear with continuous control variables
- Mixed integer linear problems when control variables are both discrete and continuous

The algorithms that are used to solve the OPF problem are broadly classified into three groups: (1) Conventional optimization methods such as Linear programming, Quadratic programming etc., (2) Intelligence search methods such as neural network, Evolutionary algorithms etc., and (3) Nonquantity approach to address uncertainties in objectives and constraints such as Fuzzy set applications, Analytic hierarchical process [17, 18].

2.3.1 General OPF problem formulation

The general OPF problem formulation to minimize the objective function $\mathcal{F}(x)$ is summarized as follows:

$$\begin{aligned} &\text{Minimize} && \mathcal{F}(x) \\ &\text{Subject to} && \mathrm{g}(x) = 0 \end{aligned} \tag{2.12}$$

and $h(x) \leq 0$

The optimality conditions for (2.12) can be derived by formulating the Lagrange function $\mathcal{L}$:

$$\mathcal{L} = \mathcal{F}(x) + \lambda^T \mathrm{g}(x) + \mu^T h(x) \tag{2.13}$$

The Kuhn-Tucker theorem [17] states that if $\hat{\mathrm{x}}$ is the *relative extremum* of $\mathcal{F}(\mathrm{x})$ that satisfies all the constraints of (2.10) at the same time then the vectors $\hat{\lambda}, \hat{\mu}$ that satisfy (2.14) must exist.

$$\begin{aligned} \frac{\partial \mathcal{L}}{\partial x} &= \frac{\partial}{\partial x}(\mathcal{F}(x) + \lambda^T \mathrm{g}(x) + \mu^T h(x))|_{\hat{\mathrm{x}},\hat{\lambda},\hat{\mu}} \\ &= 0 \\ \frac{\partial \mathcal{L}}{\partial \lambda} &= \mathrm{g}(x)|_{\hat{x}} = 0 \\ diag\{\mu\}\frac{\partial \mathcal{L}}{\partial \mu} &= diag\{\mu\}\,\mathrm{h}(x)|_{\hat{x},\hat{\mu}} = 0 \\ \hat{\mu} &\geq 0 \end{aligned} \tag{2.14}$$

It is the goal of OPF algorithms to find a solution point $\hat{x}$ and corresponding vectors $\hat{\lambda}, \hat{\mu}$ that satisfy the above conditions.

2.3.2 Classification of OPF algorithms

OPF algorithms are classified mainly into classes [17] considering the fact that very powerful methods exist for power flow that provide an easy access to intermediate solutions in the course of iteration process. The following are the two classes of OPF.

- **Class A:** In this class, the optimization starts from a solved power flow. The Jacobian and other sensitivity relations are used in optimizing process. The process as a whole is iterative and after each iteration the power flow equations are solved anew.
- **Class B:** In this class, power flow relations are attached as equality constraints for methods relying on the exact optimality conditions. There is no prior knowledge of load flow solution. Load flow study is a steady-state analysis whose target is to determine the voltages, currents and real and reactive power flows in the system. The process

is iterative and each intermediate solution approaches the power flow solution.

There are advantages and disadvantages in both methods, which have a certain bearing depending on the objective, the size of the problem and the envisaged application.

2.3.3 The Interior Point Method (IPM)

Several strategies were proposed in [19] for an OPF with active power dispatch and voltage security using an IPM that proved to be robust. The majority of the IPM implementations for solving market problems and power system security constraints use linear programming techniques. In [20], use of IPM for non-linear problems using Newton's direction method and Merhotra's predictor-corrector was explained. The latter method reduces the number of iterations to obtain the final solution. Non-linear optimization techniques were also used to address a variety of voltage stability issues, such as the maximization of loading parameters in voltage collapse studies as explained in [21] and [22].

Further details of OPF for maximization of distance from voltage collapse and the methodology/work flow adopted in this thesis are explained in detail in chapter 5.

Chapter 3

3. PROPOSED VOLTAGE STABILITY INDEX

Voltage instability phenomena can be identified by both static and dynamic analysis. However, when only time-series from dynamic simulation is available, it is necessary to identify an equivalent from the time-series of the simulations. The choice of the model used was made by considering the constraint between model accuracy, speed to compute the stability limits and the fact that no other information about the power system other than the time series was available.

3.1 Equivalent Models

Simple equivalent models of the power system and the load at the measurement point are estimated from the data, and are then used for calculating the PV curves to predict the stability limits [10, 23].

3.1.1 Single Voltage Source Model

A Thevenin equivalent of the power system as viewed from the measurement point can be constructed as shown in figure 3.1. Thevenin equivalent network is computed based on Thevenin's theorem, which states that any combination of sinusoidal AC sources and impedances with two terminals can be replaced by a single voltage source and single series impedance as shown in 3.1. Further details can be found in [6].

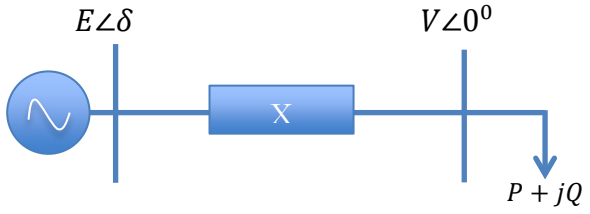

Figure 3.1 Equivalent model

Here we assume that the network resistances can be neglected. The equivalent model parameters (E, δ, X) are calculated from the time series data as shown below.

$$P = \frac{EV}{X}\, sin\delta, \qquad Q = \frac{V(Ecos\delta - V)}{X} \tag{3.1}$$

'm' samples at any instant of time yields:

$$\begin{matrix} P_iX - V_iEsin\delta_i = 0 \\ , i = 1, \ldots, \\ Q_iX - V_iEcos\delta_i + V_i^2 = 0 \end{matrix} \tag{3.2}$$

Only $m + 2$ variables are unknown with $2m$ equations in (3.2). Equation (3.2) is thus overdetermined, and the model parameters can be estimated by solving the following least squares problem:

$$\underset{E, X, \delta_i}{min} \left\| \begin{matrix} P_1X - V_1Esin\delta_1 \\ Q_1X - V_1Ecos\delta_1 + V_1^2 \\ . \\ . \\ . \\ P_mX - V_mEsin\delta_m \\ Q_mX - V_mEcos\delta_m + V_m^2 \end{matrix} \right\| \tag{3.3}$$

3.1.2 Load Model

The equation of the considered linear P-Q load model is given by $Q = \alpha + \beta P$. The values of α and β are calculated by solving the least square problem shown in (3.4).

$$\underset{\alpha, \beta}{min} \left\| \begin{bmatrix} 1 & P_1 \\ . & . \\ 1 & P_m \end{bmatrix} \begin{bmatrix} \alpha \\ \beta \end{bmatrix} - \begin{bmatrix} Q_1 \\ . \\ . \\ Q_m \end{bmatrix} \right\| \tag{3.4}$$

This linear P-Q load model can be combined with the single voltage source model in order to calculate the PV curve and the voltage stability limit for the power transfer at the bus of interest by solving (3.5).

$$P^2X^2 - E^2V^2 + (\alpha X + \beta PX + V^2)^2 \tag{3.5}$$

3.2 Three Layer Severity Index

The proposed Voltage Stability (VS) index provides a measure of how far the system is from the maximum loadability limit. The three layers of the index are:

- Single Bus Index (SBI)
- All Buses Index (ABI)
- Global Bus Index (GBI)

The SBI is a $R^{(2Nb \times b)}$ matrix where Nb is the number of buses under analysis as shown in (3.6). The SBI provides the distance in pre-and-post contingency (PV space) for each load power consumption to the power (P_{lim}) and voltage (V_{lim}) limits of a selected bus or group of buses. SBI is defined in (3.6) and is divided as follows: columns 1 to 3 correspond to the distance from each of the given loading levels to the limit with respect to power while column 4 to 6 corresponds to the distance for each loading level to the limit with respect to the voltage. In SBI, for each bus there are four rows in which odd rows corresponds to pre-contingency data and even rows corresponds to post-contingency data. First row and second row corresponds to pre-contingency curve-1 and post-contingency curve with respect to pre contingency curve-1 respectively. While third and fourth row corresponds to pre-contingency-2 and post-contingency curve with respect to pre contingency curve-2 respectively

$$SBI = \left[\begin{array}{cccccc|cccccc}
sb_{(1,1)} & sb_{(1,2)} & sb_{(1,3)} & sb_{(1,4)} & sb_{(1,5)} & sb_{(1,6)} \\
sb_{(2,1)} & sb_{(2,2)} & sb_{(2,3)} & sb_{(2,4)} & sb_{(2,5)} & sb_{(2,6)} \\
sb_{(1',1)} & sb_{(1',2)} & sb_{(1',3)} & sb_{(1',4)} & sb_{(1',5)} & sb_{(1',6)} \\
sb_{(2',1)} & sb_{(2',2)} & sb_{(2',3)} & sb_{(2',4)} & sb_{(2',5)} & sb_{(2',6)} \\
\hline
\vdots & \vdots & \vdots & \vdots & \vdots & \vdots \\
\hline
sb_{(n,1)} & sb_{(n,2)} & sb_{(n,3)} & sb_{(n,4)} & sb_{(n,5)} & sb_{(n,6)} \\
sb_{(m,1)} & sb_{(m,2)} & sb_{(m,3)} & sb_{(m,4)} & sb_{(m,5)} & sb_{(m,6)} \\
sb_{(n',1)} & sb_{(n',2)} & sb_{(n',3)} & sb_{(n',4)} & sb_{(n',5)} & sb_{(n',6)} \\
sb_{(m',1)} & sb_{(m',2)} & sb_{(m',3)} & sb_{(m',4)} & sb_{(m',5)} & sb_{(m',6)}
\end{array}\right] \quad (3.6)$$

$$sb_{(i,j)} = \frac{P_{i,lim} - P_{i,j}}{P_{i,lim}}, \qquad sb_{(i,k)} = \frac{V_{i,lim} - V_{i,j}}{V_{i,lim}},$$

$$sb_{(i',j)} = \frac{P_{i',lim} - P_{i',j}}{P_{i',lim}}, \qquad sb_{(i',k)} = \frac{V_{i',lim} - V_{i',j}}{V_{i',lim}},$$

$$sb_{(r,j)} = \frac{\hat{P}_{r,lim} - \hat{P}_{r,j}}{\hat{P}_{r,lim}}, \qquad sb_{(r,k)} = \frac{\hat{V}_{r,lim} - \hat{V}_{r,j}}{\hat{V}_{r,lim}},$$

$i = 1,4,7,9 \ldots., n \qquad j = 1,2,3$

$i' = 2,5,8,10.., n' \qquad j = 1,2,3$

$r = 3,6,9,12 \ldots., m \qquad k = 4,5,6$

$m = 2Nb \qquad n = m - 1$

$m' = 2Nb \qquad n' = m' - 1$

If an element of SBI is negative, then the power or the voltage at the some loading level has exceeded the operational limits. It should be noted that the voltage and power limits considered are not the theoretical maximum loadability limits but the operational limits i.e. a ϵ smaller than the theoretical limits. ϵ is set to the best judgement of the analyst, e.g. $\mathrm{P_{max}} = \mathrm{P_{max}} - \epsilon \mathrm{P_{max}}$. Since in real power system, the operational limits is lesser than the theoretical limits because they are based on other factors like thermal rating of the transmission line.

The All Bus Index ABI is a $\mathrm{R}^{(1\times 6)}$ vector with the loading points of the bus which has the minimal distance to the power and voltage limits in pre-and post-contingency is shown in (3.7).

$$ABI = \left[\Delta\hat{P}_{a(1,1)} \quad \Delta\hat{P}_{b(1,2)} \quad \Delta\hat{P}_{c(1,3)} \quad \Delta\hat{V}_{a(1,1)} \quad \Delta\hat{V}_{b(1,2)} \quad \Delta\hat{V}_{c(1,3)}\right] \quad (3.7)$$

$$\Delta\hat{P}_{(1,j)} = min\left\|\begin{matrix}\Delta P_{i,j} \\ \Delta\hat{P}_{r,j}\end{matrix}\right\|, \qquad \Delta\hat{V}_{(1,k)} = min\left\|\begin{matrix}\Delta V_{i,k} \\ \Delta\hat{V}_{r,k}\end{matrix}\right\|$$

Where $\mathrm{i}, \mathrm{j}, \mathrm{r}$ and k are defined below (3.6).

The Global Bus Index GBI is a vector with 2 entries that provides the shortest distance to the power and voltage limits with respect to all the buses as show in (3.8).

$$GBI = [\Delta\bar{P} \quad \Delta\bar{V}] \tag{3.8}$$

$$\Delta\bar{P} = min\left|\Delta\hat{P}_{a(1,1)} \quad \Delta\hat{P}_{b(1,2)} \quad \Delta\hat{P}_{c(1,3)}\right|,$$

$$\Delta\bar{V} = min\left|\Delta\hat{V}_{a(1,1)} \quad \Delta\hat{V}_{b(1,2)} \quad \Delta\hat{V}_{c(1,3)}\right|$$

3.3 Voltage Stability (VS) Index Computation

This index is developed as part of the project FP7 iTesla [24]. This project aims to build a software toolbox. The off-line analysis workflow within iTesla toolbox does the dynamic impact assessment of the detailed time domain simulations. The iTesla toolbox can run time domain simulation continuously for only one time. So, this index is developed in a way to comply with the requirements of iTesla toolbox.

3.3.1 Assumptions

In this new method, only one set of time domain simulation is considered as input to the VS index. The time domain simulation consists of a one pre-contingency operating state followed by three or more post-contingency operating states as shown in figure 3.2. A minimum of three operating points are required to estimate the PV curve for a particular network configuration. Information of only one operating point is available from time domain simulations for pre-contingency state.

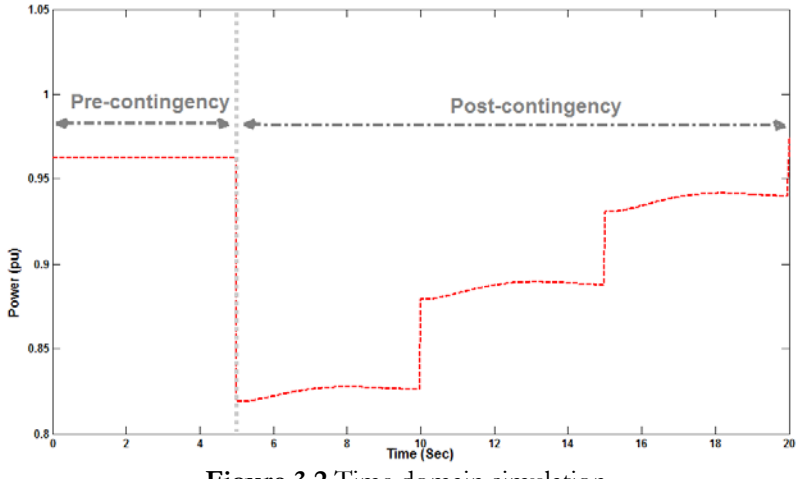

Figure 3.2 Time domain simulation

So, the remaining two operating points are given as input by the operator. Information about the no-load operating point (V_o, P_o), operational point

based on voltage limits (V_{lim}, P_1) & MVA limits (V_2, P_{lim}) of the line for pre-contingency state are given as input to the program by the operator. Based on these operating points two PV curves can be estimated for pre-contingency state as shown in figure 3.3. The exact solution exists between these two PV curves.

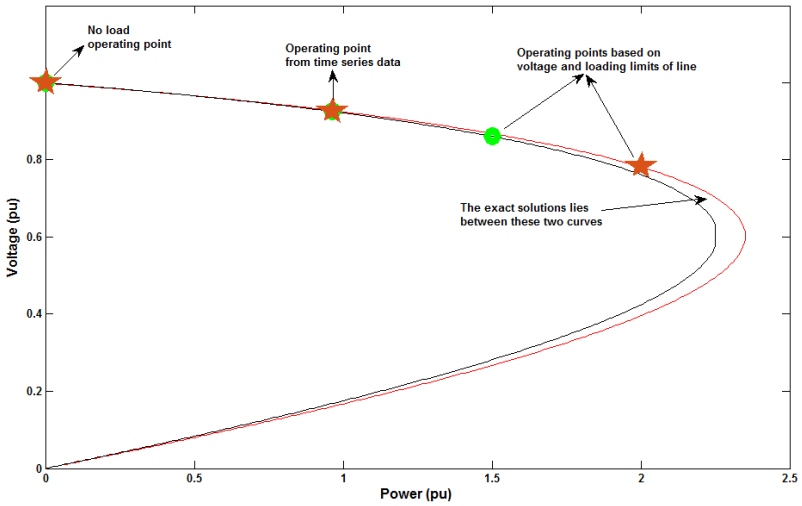

Figure 3.3 Pre-contingency PV curve estimation

3.3.2 Summary of the voltage stability index computation method

The following flow chart explains the execution sequence of the VS severity index computation.

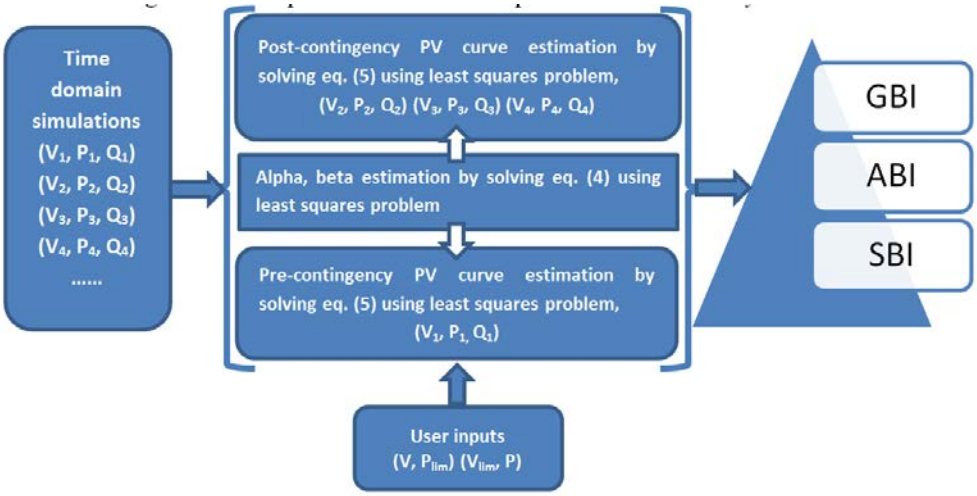

Figure 3.4 Index computation flow chart

In the new method, the VS severity index is computed in the following steps.

1. The information from time domain simulation is divided into pre-and-post contingency states.
2. Using the post-contingency operation states (P_i, Q_i) from time series data, (α, β) are estimated by solving (4).
3. Using the estimated (α, β) values and (V_i, P_i) from time series data, the PV curve is estimated by solving (5) using least square problem.
4. Using the data (V_1, P_1, Q_1) from time series and the input values based on no load operating point (V_o, P_o), operational point based on voltage limits (V_{lim}, P_1) & MVA limits (V_2, P_{lim}) of the line, the PV curve is estimated by solving (5) using least square problem.
5. Based on the estimated PV curves and input operation states the severity indices are calculated as explained in Section-2.

3.4 Index Computation using synthetic simulations

This section illustrates the use of the proposed index as described in the above sections and interpretation of its results. The aim is to calculate the distance from different operating points in pre-and-post contingency state to the maximum operational limits in terms of voltage and power.

For this illustrative example a simple two-bus system connected with two lines as described in figure 3.1 was used. Time domain simulation was done for duration of 20 seconds. Contingency was applied at 5th sec and load perturbations applied for every five seconds until the end of simulation. The time domain simulation with Voltage and Power along time axis is shown in Figure 3.5 and the estimated post-contingency PV curve is shown in Figure 3.6.

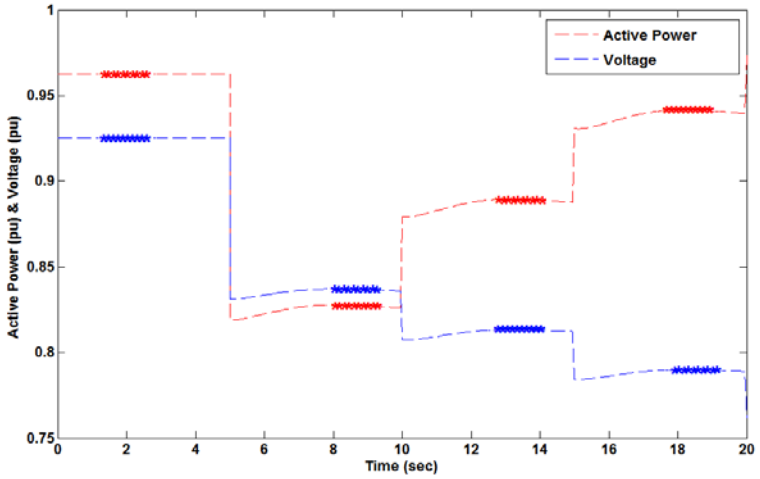

Figure 3.5 Set of simulations and data required to calculate the index

The red colour points in the figure 3.6 are the sampled values from time series data and blue colour curve is the estimated PV curve.

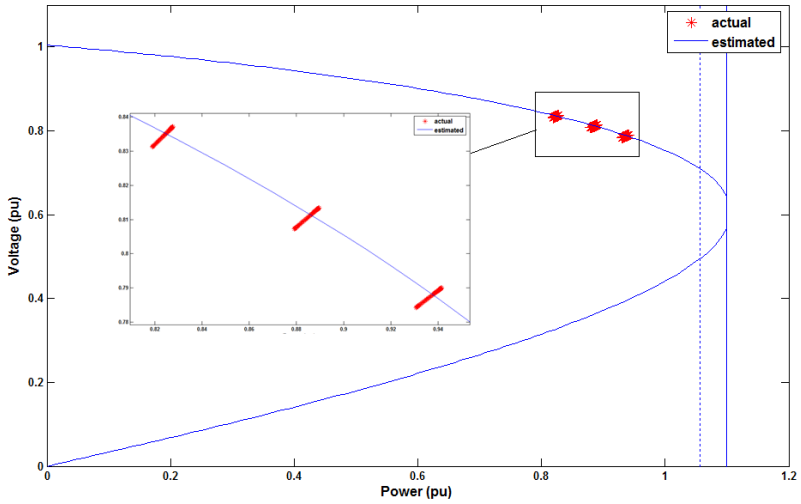

Figure 3.6 Estimated post-contingency PV curve

Figure 3.7 (a) and (b) depicts the estimated post contingency curve with respect to estimated pre-contingency curves. These curves were estimated using the blue and red sections highlighted in figure 3.5 which are shown as brown colour points on pre-contingency curve and red color points on post-contingency curve.

(a) Post-contingency with respect to pre-contingency curve-1

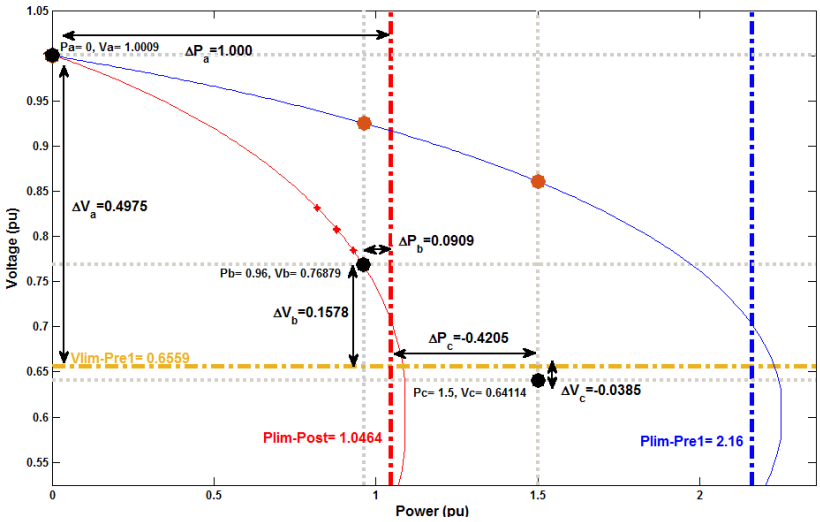

(b) Post-contingency with respect to pre-contingency curve-2

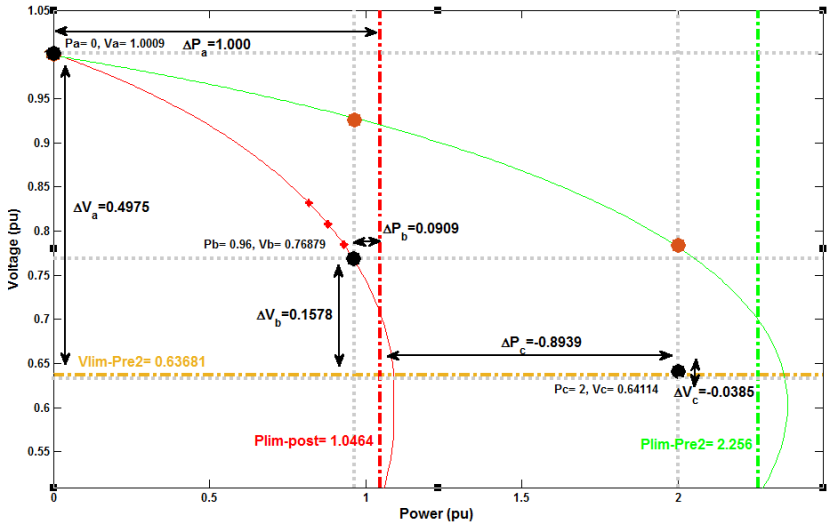

Figure 3.7 Estimated PV curves using pre-and-post fault data

It can be observed from figure 3.7 that the post-contingency curve (red) is smaller than the pre-contingency curves (blue, green) because the impedance of the system increased after the disturbance in the network at 5th sec. It should also be noted that the distances ($\Delta P's\ and\ \Delta V's$) in the post-contingency are smaller than in pre-contingency curves and negative in some cases. In post-contingency the curve shrinks and the power limit decreases.

Table 3.1 Voltage stability indices for the synthetic case

			$\Delta\bar{P}$	$\Delta\bar{V}$		
GBI			**-0. 8939**	**-0.0385**		
	$\Delta\hat{P}_a$	$\Delta\hat{P}_b$	$\Delta\hat{P}_c$	$\Delta\hat{V}_a$	$\Delta\hat{V}_b$	$\Delta\hat{V}_c$
ABI	1.0000	0.0909	**-0.8939**	0.4975	0.1578	**-0.0385**
	ΔP_a	ΔP_b	ΔP_c	ΔV_a	ΔV_b	ΔV_c
SBI B_{11}	1.0000	0.5543	0.3056	0.5249	0.4110	0.3124
SBI $\hat{B}_{11}$	1.0000	0.0909	-0.4205	0.4975	0.1578	-0.0385
SBI B_{12}	1.0000	0.5733	0.1135	0.5707	0.4533	0.2302
SBI $\hat{B}_{12}$	1.0000	0.0909	**-0.8939**	0.4975	0.1578	**-0.0385**

After estimating the equivalent model, the index described in the above section is computed and the results are shown in table 3.1. GBI is used to interpret the given operating point that is very near to the voltage stability limits of the system. In this case, both the elements of GBI are negative indicating that at least one power and voltage limit was violated. ABI is used

to retrieve more specific information i.e. in this case elements (1, 3) and (1, 6) of the given load levels are negative indicating that there are violations at heavy loading level in both power and voltage. From SBI it can be observed that elements (4, 3) and (4, 6) are negative indicating that during post-contingency these loading levels are on the right hand side of the power limit and below the voltage limit as shown in figure 3.7(a) and 3.7(b). Thus, from severity index it can be interpreted that operation of the system at this loading level will lead voltage instability in case of this contingency.

Chapter 4

4. A METHOD FOR VOLTAGE STABILITY ASSESSMENT USING DECISION TREES

In this chapter, the proposed approach and workflow to create and use decision trees for voltage stability assessment is explained in detail.

4.1 Attribute selection for the DTs

In this thesis, load active powers and voltages are considered as attributes for splitting the data because they are one of the important factors in assessing the voltage stability of the system. From the definitions of different voltage instabilities explained in chapter 2, it can be observed that systems inability to cater the power demand of the load is one important reason for voltage instability. A power system is designed to supply power to the loads and the knowledge of systems capability to cater load requirements/increments in different network configuration can help the operator to understand the state of the system and foresee the consequences for different load requirements. The chosen attribute should be such that it can discriminate between different system conditions. For example, the voltage of a voltage controlled bus is a bad attribute as it hardly changes, while voltages and angles of the buses that are electrically distant from the generators (eg. radially connected loads with high impedance) are good attributes for stability classification. Thus, load active powers and voltages are used as attributes to build the decision trees that can aid the power system operator with voltage stability assessment for different load power consumptions and network configurations.

4.2 Workflow

The workflow adopted to build a decision tree for the selected network is shown in figure 4.1. Initially, a network for study is selected and the loads are assumed to be constant PQ loads in this thesis.

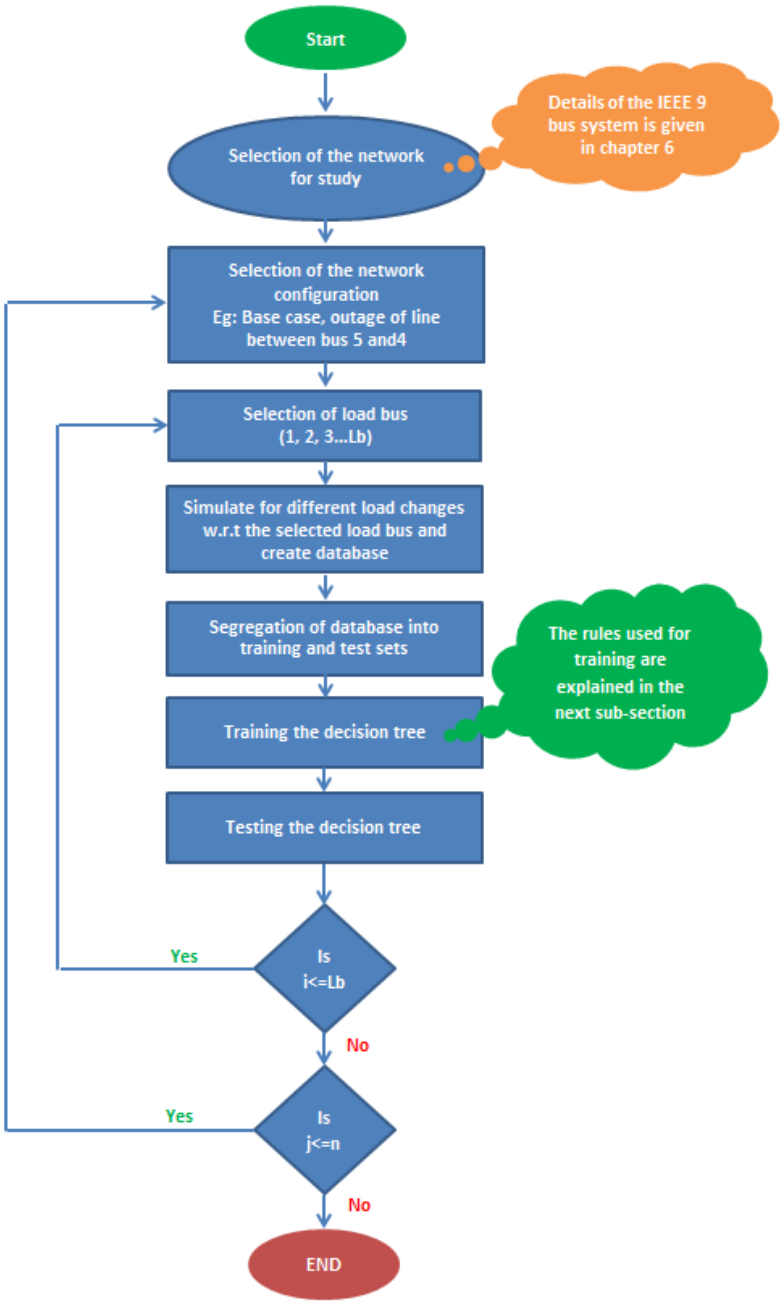

Figure 4.1 Workflow for creation of decision tree

For each topology, such as the base case and after different contingencies, a database is created with the load flow results for different load power consumptions. These databases are then used to build the decision trees that are used to predict the voltage stability of the considered system using measured load powers and voltages.

It is possible that the data obtained from simulated environment lack the exact representation of the system state and may be biased with respect to the assumptions like load variations, scenarios etc. For example in this thesis, all the loads are assumed to be constant PQ loads in the system, which is not the case in a real power system. The loads in a real power system are quite diversified because it contains devices like refrigerators, pumps, heaters, lamps etc. For example the refrigerator power consumption varies with respect to compression process and temperature absorption process but a PQ load consumes constant amount of power.

Moreover the load composition changes based on weather, time and economy. Hence, it is complicated and time consuming to represent individual load characteristics for large scale system studies. The advantages of having simulated data is the accessibility to get variety of data within a very short span of time which is not the case for real time data, interpret the response of the system in case of a fault which happens seldom in real system and low cost and low risk environment to try all the possible scenarios etc.

Data is required to train and test a decision tree. The training set is used to build the decision tree and the test set is used to check accuracy of the decision tree. Depending upon the availability of data, there are various procedures as cross validation, leave one out and bootstrap to use for model validity [12].

4.2.1 Input for the DTs

The DTs are created with respect to every load bus for different network configurations. The number of DTs created is therefore proportional to number of load buses and topologies considered. The number of branches for a tree increases with increase in data. Creating one tree for a network configuration increases the size of the tree that further complicates interpretation. Moreover, creating one tree for a network configuration increases the computational burden and lookup time.

For these reasons every network configuration will have a tree with respect to every load bus. Load flow simulations are done for different network configuration with several load variations that are then used to train and test the decision tree for that network configuration.

4.2.2 Voltage Stability classification for training the DTs

Publications based on DT applications to power systems were provided in [25]. According to [15, 25], there is no standard universal approach for voltage stability classification using DTs. The region of operation is classified to "stable" and "unstable". The disadvantage of classifying the region of operation to only "stable" and "unstable" is that if the system is operating in the boundary of these regions, the decision tree trained on this data identifies the current operating point in "stable" region. In order to avoid this problem, the region of operation in this thesis is classified to four regions. They are the "stable within grid limits", "stable outside grid limits", "marginally stable" and "unstable" regions. Initially, the Euclidean distance is calculated for the given load operating point i with respect to load bus a (considering loads at bus a, b and c) (Pa_i, Pbc_i) from nearest unstable point (Pa_{nSNB}, Pbc_{nSNB}) using (4.1).

$$Distance = \sqrt{(Pa_{nSNB} - Pa_i)^2 + (Pbc_{nSNB} - Pbc_i)^2} \quad (4.1)$$

Margin is calculated as given in (4.2).

$$Margin = \frac{Distance}{Pa_i + Pbc_i} \quad (4.2)$$

If (4.2) is less than 25%, then the region of operation is classified as "marginally stable" region. If the available margin is greater than or equal to 25% with voltages at all the load buses being greater than 0.95 pu (per unit is the expression of system quantities as fractions of a defined base unit quantity. Further details about per unit can be found in [26]), then the region is classified as "stable within grid limits" region, otherwise it is classified as "stable outside grid limits" region. If the given load operating point is the saddle node bifurcation point or it exists further away from the given saddle node bifurcation point, then the region is classified as being in the "unstable" region. The classification criteria are visualized in figure 4.2.

The given load flow outputs are classified in to the regions based on the conditions explained above. The trained decision trees are tested with the test set and the accuracy of the classification is calculated. Low accuracy in classification indicates that the decision tree is not trained properly and it is needed to be retrained.

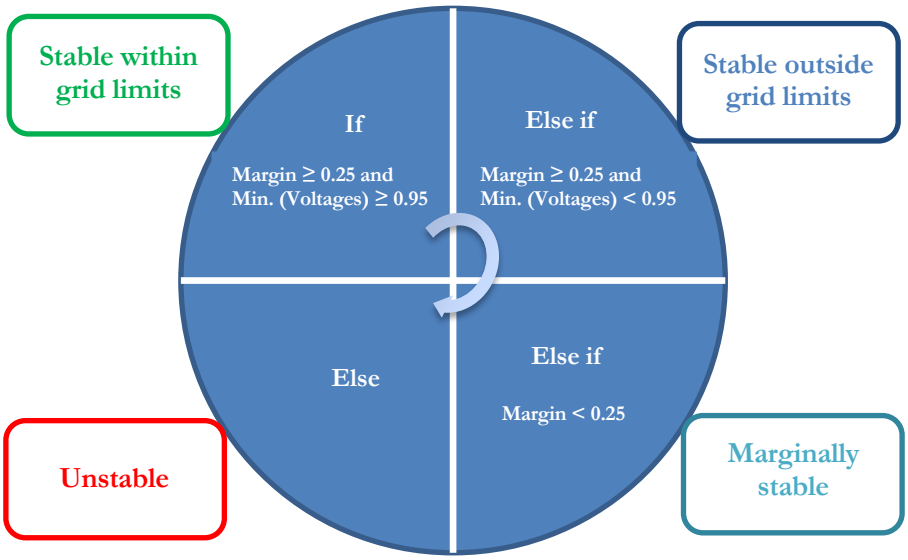

Figure 4.2 The classification criteria used

These classification rules were also used to verify the classification of time domain simulation output by the created trees. The results are provided and explained in chapter 6.

Chapter 5

5. A METHOD FOR LOOKING UP PRE-CALCULATED PREVENTIVE ACTIONS AGAINST VOLTAGE PROBLEMS

In this chapter, the proposed approach and workflow used to generate optimal power flow solutions is explained in detail.

5.1 OPF with Voltage Stability Constraints – Maximization of the Distance from Collapse

In this OPF problem, maximization of the distance between the current value of the loading parameter and its value at the voltage collapse point is considered as objective function. Therefore as the system moves towards the bifurcation point more weight is given to the voltage stability when compared to the generation cost. In this thesis, the following optimization problem that is available in Power System Analysis Toolbox (PSAT) [27] is used to generate OPF solutions to the operating points. This optimization problem represents the system security through use of voltage stability conditions. It is based on interior point method proposed in [20] and OPF formulations for maximizing the distance from voltage collapse proposed in [21] and [22].

$$\text{Max. } G = \lambda \tag{5.1}$$

$$
\begin{aligned}
\text{S.t} \quad & (\delta, V, Q_G, P_S, P_D) = 0 && \rightarrow \text{PF equations} \\
& g^c(\delta^c, V^c, Q_G^c, \lambda_c, P_S, P_D) = 0 && \rightarrow \text{Max load PF equations} \\
& \lambda^{min} \le \lambda \le \lambda^{max} && \rightarrow \text{Loading margin} \\
& P_S^{min} \le P_S \le P_S^{max} && \rightarrow \text{Supply bid blocks} \\
& P_D^{min} \le P_D \le P_D^{max} && \rightarrow \text{Demand bid blocks} \\
& \phi_{ij}(\delta, v) \le \phi_{ij}^{max} && \rightarrow \text{Flow limits} \\
& \phi_{ji}(\delta, v) \le \phi_{ji}^{max} \\
& \phi_{ij}(\delta^c, v^c) \le \phi_{ij}^{max} \\
& \phi_{ji}(\delta^c, v^c) \le \phi_{ji}^{max} \\
& Q_G^{min} \le Q_G \le Q_G^{max} && \rightarrow \text{Gen. } Q \text{ limits}
\end{aligned}
$$

$$Q_G^{min} \le Q_G^c \le Q_G^{max}$$
$$V^{min} \le V \le V^{max} \qquad \rightarrow V \text{ security limits}$$
$$V^{min} \le V^c \le V^{max}$$

Constants:

$P_{S_{max_i}}$ upper limit of the energy bid offered by unit i

$P_{S_{min_i}}$ lower limit of the energy bid offered by unit i

$P_{D_{max_j}}$ upper limit of the energy bid demanded by consumer j

$P_{D_{min_j}}$ lower limit of the energy bid demanded by consumer j

λ the loading margin

An electricity market is a system enabling purchases (bidding), sales and short-term trades generally in the form of financial or obligation swaps. Energy bids are the tenders for purchasing energy from different generations in the electricity markets. Market bidding is the process of purchasing electricity in electricity markets [28].

In this case, a second set of power flow equations and constraints with a superscript c is introduced to represent the system at critical conditions associated with the loading margin λ that drives the system to its maximum loading condition. The critical power flow equations g^c can present a line outage. The maximum or critical loading point could be either associated with violation of either a thermal (thermal limits are not considered in this thesis) or a bus voltage limit or being at the voltage stability limit (saddle-node point) corresponding to a system singularity. Thus, for the current operation point and maximum loading, the generator and load powers are defined as, respectively

$$\begin{aligned} p_G &= p_G^0 + p_S \\ p_L &= p_L^0 + p_D \\ p_G^c &= (1 + \lambda + k_G^c) p_G \\ p_L^c &= (1 + \lambda) p_L \end{aligned} \tag{5.2}$$

Where p_G^0 and p_L^0 stand for generator and load powers which are not part of market bidding and k_G^c represents a scalar variable which distributes system losses associated depending up on the power injection by the generators i.e. a generator injecting more power in to the grid contributes more power for losses than the generator injecting less power. It is assumed that losses corresponding to maximum loading level defined by λ in (5.1) are distributed among all the generators depending on the power injection by the corresponding generators in to the grid.

5.2 Application of OPF

In this thesis, OPF with voltage stability constraints and distance from saddle node bifurcation point is applied to find optimal operating points to the operating points in "stable outside grid limits" or "marginally stable" region. It is implemented in this way because all these OPF solutions are grouped in to a database with operating points mapped to their corresponding OPF solutions. This database is used for searching the OPF solution of nearest operating point. Further details are explained in the following sub-sections.

5.2.1 Workflow execution

In the first step of the workflow, the current load operating points (P, V) is given as an input to the trained DTs to identify the region of operation. If the output from DTs is "stable outside grid limits" or "marginally stable" then workflow proceeds to the OPF section, otherwise it proceeds to next load operating point that is needed to be classified. In the OPF section, the given objective function of maximizing the distance from voltage collapse is solved for a solution satisfying the conditions explained in section 5.1. If OPF fails to find a solution for the satisfying the given conditions, then the following conditions are relaxed in the given order of preference.

1. Acceptable minimum voltage level is decreased from 0.95 pu in steps of 0.01 up to 0.85 pu.
2. Removal the voltage limits.
3. Reduction in the load active power and reactive power (load shedding).

The work flow used to generate OPF solutions is shown in figure 5.1.

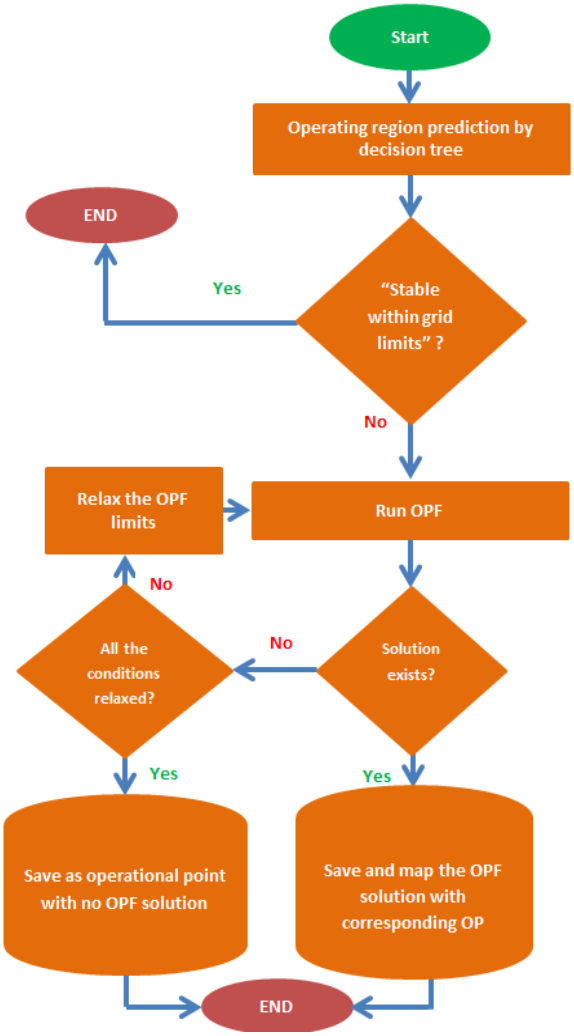

Figure 5.1 Workflow for creating OPF solutions

The active power direction for load reduction is given in (5.3)

$$P_D = \frac{-Pa_i}{\|Pa_i+Pb_i+Pc_i\|} \tag{5.3}$$

where Pa, Pb and Pc are the load active powers for the given load operating point "i". Similarly, the reactive power direction is given by replacing the load active powers in (5.3) with load reactive powers. If OPF fails to find a solution even after relaxing the conditions then it is saved as an operating point with no OPF solution. All these solutions obtained from OPF are being mapped to from their corresponding operational points. So, when the DTs identify the state of the system as "stable outside grid limits" or 'marginally

stable', the algorithm searches for nearest operating point in database and applies its OPF solution to the system.

5.2.2 Database of OPF solutions

All the operating points that are simulated are mapped with their OPF solutions and are made into a database. The block diagram in figure 5.2 explains how these OPF solutions are used.

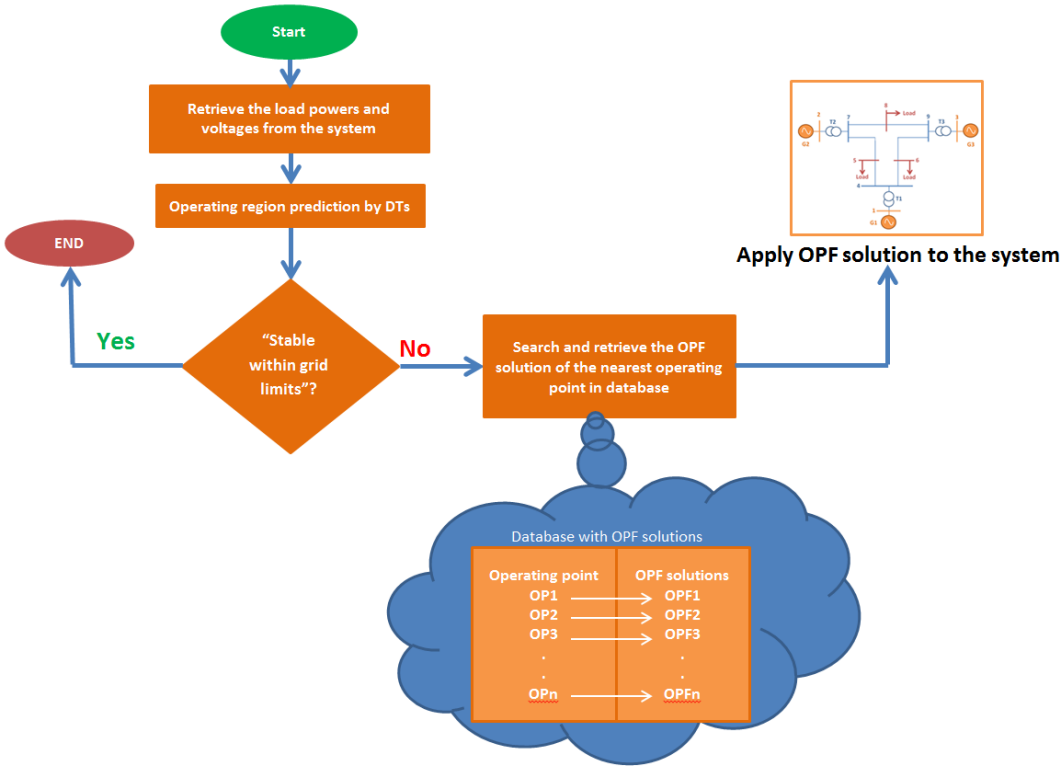

Figure 5.2 Workflow showing the usage of OPF solutions from database

From the figure 5.2, it can be observed that the current load active power and voltages from the system are given as inputs to the created DTs (DTs created from the training set). If these DTs classify the system operation in "outside grid limits" or the "marginally stable" region, the algorithm searches for the nearest operating point in the database and will then retrieve the OPF solution of the nearest operating point. This OPF solution is applied to the system by rescheduling the generating units and/or doing load shedding in order to improve the state of the system.

5.2.3 Significance of the proposed approach

The advantage of the proposed method can be highlighted with respect to the time taken to retrieve the OPF versus online OPF calculation. It can be explained by considering exponential recovery loads. Exponential recovery loads are given by (5.4)

$$\dot{x}_p = \frac{-x_p}{T_p} + P_s + P_t \tag{5.4}$$

where x_p is the state variable for the load active power, P_s and P_t are the static and transient real power absorptions, which depend on load voltage as given in (5.5). T_p is the active power time constant.

$$P_s = P^0 \left(\frac{V}{V^0}\right)^{\alpha_s}$$
$$P_t = P^0 \left(\frac{V}{V^0}\right)^{\alpha_t} \tag{5.5}$$

where α_s and α_t are the static and transient active power exponents and V^0 is the voltage at the load bus from the load flow solution. Similar equations hold for reactive power. The response of the exponential recovery load for an outage of one of the two available transmission lines in a simple two bus system is shown in figure 5.3. The response of the load after the event (overshoot/undershoot) depends on α_t. The time taken to recover the load power consumption to the value (load power consumption before the event) before the occurrence of the event depends active power time constant. If $\alpha_t = 0$, there will be load undershoot. For the values of $\alpha_t < 0$, there will be load overshoot and for the values of $\alpha_t > 0$, there will be load undershoot. The undershoot for $\alpha_t > 0$ is more than the undershoot for $\alpha_t = 0$ and the same can be observed in figure 5.3.

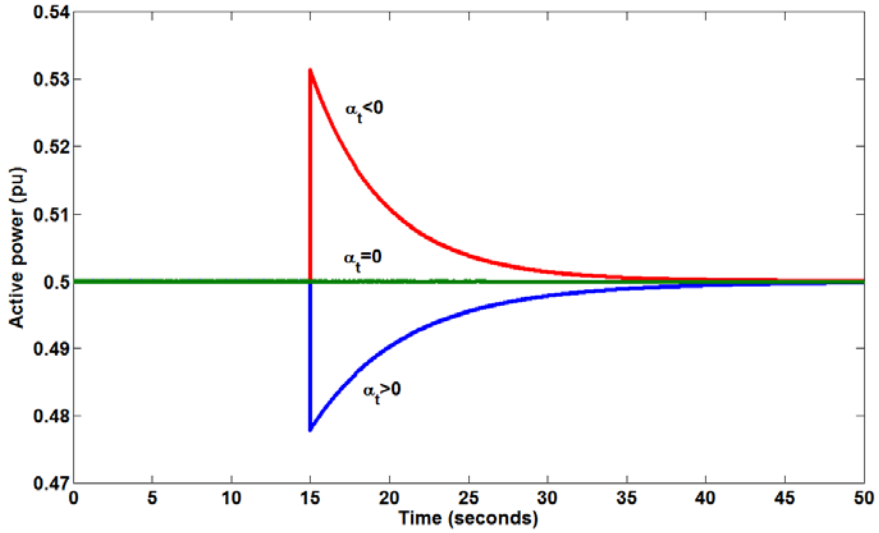

Figure 5.3 Active power response of exponential recovery load for outage of the line in two bus system

It should be noted that when $\alpha_t = 0$, from (3.5) active power $P_t = P^0$ and reactive power $Q_t = Q^0$. This indicates that the load acts as a constant PQ load. The same can be observed in figure 5.3. Similarly, when $\alpha_t > 0$ i.e. $\alpha_t = 1$ or $\alpha_t = 2$ it acts as constant current or constant impedance load respectively. Load models, where active and reactive powers vary directly with the voltage magnitudes are known as Constant current loads. Nonlinear load models, where active and reactive powers vary with square of the voltage magnitude are known as Constant impedance loads.

For $\alpha_t > 0$ before the load recovers, by using this proposed approach it would take less time to search for OPF solution of nearest operating point and apply to the power system before it becomes unstable. The idea of this approach is that, by using this proposed approach it would take less time to identify the state of the system and apply OPF solution after the contingency than to compute the OPF solution online. The time taken to retrieve the OPF solution from database versus the time taken to calculate OPF solution online is investigated in the case studies of chapter 6.

Chapter 6

6. CASE STUDIES

In this chapter, the results obtained from the proposed approach (explained in chapters 3, 4 and 5) on the test system are provided and explained in detail.

6.1 Background

The main objective of this case study was to demonstrate the use of decision trees and offline computed OPF solutions for early identification of voltage instability and suggest remedial actions. This proposed approach was tested on the IEEE 9 bus system. Computer simulations were carried out on this system for different loading conditions and different network configurations.

The simulation of IEEE 9 bus system for different loading conditions and network configurations was performed in PSS/E. The simulations in PSS/E were automated by a Python script. Machine learning toolbox in MATLAB was used to train and test the decision trees on this simulation results obtained from PSS/E. OPF was performed using Power System Analysis Toolbox (PSAT) [22], a program that operates in MATLAB numerical computing environment. Finally, a MATLAB script was written to validate the created decision trees and the computed OPF solutions by generating random load powers.

6.2 Inputs

This section presents the process of selecting appropriate input data for the case study, with an emphasis on the need of the data and models used, to accurately describe the power system.

6.2.1 General Inputs

The power system data for the case study was in the formats used by PSS/E and PSAT. Therefore, power system data (Transmission line impedances, Transformer impedances, generator ratings and exciter types) in both the files

was verified manually and care was taken to make the power flow converge to the same bus voltage magnitudes and angles for both the files.

- The loads are assumed to have no dynamic components and are modeled as consuming constant power under a constant power factor.
- Simulations were performed for different loading conditions with respect to every load bus for different network configurations.

6.2.2 Test system

The IEEE 9 bus system represents a simple approximation of the Western System Coordinating Council (WSCC) to an equivalent system with nine buses and three generators as shown in figure 6.1. The system data was available in PSS/E and PSAT.

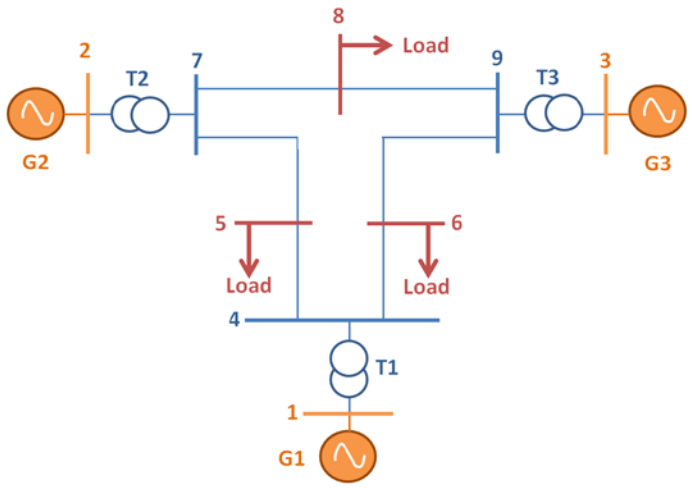

Figure 6.1 Single Line Diagram of IEEE 9 bus system

This test system consists of 9 buses, 3 generators, 3 two-winding transformers, 6 transmission lines and 3 loads. The voltage level of the transmission system is 230 kV and the voltage levels of the generators 13.8, 16.5 and 18 kV. Further generator data is given in table 6.1.

Table 6.1 Generator data

Gen. Bus No.	Voltage (kV)	Type	Generator*	Exciter*	Turbine Governor*	Stabilizer*
1	16.5	Swing	GENSAL	IEEE T1	IEESGO	PSS2A
2	18.0	PV	GENROU	IEEE T1	IEESGO	PSS2A

3	13.8	PV	GENROU	IEEE T1	IEESGO	PSS2A

*-detailed values of each type are given in Appendix.

6.2.3 Simulated network configurations

Load flow studies were conducted by varying the load demand at the load buses. These simulations were automated using a python script. Data was generated for different network configurations with respect to every load. Apart from the base case where all the transmission lines are in service, the following network configurations were also simulated.

- Outage of line between Bus 4 and 5
- Outage of line between Bus 5 and 7
- Outage of line between Bus 4 and 6
- Outage of line between Bus 6 and 9
- Outage of line between Bus 7 and 8
- Outage of line between Bus 8 and 9

For the above mentioned network configurations, power flow simulations were conducted for load variations with respect to every load. For the above mentioned network configurations, power flow calculations were conducted for Load variations with respect to load 5, load 6 and load 8. On an average, each network configuration has 100,000 simulated operational points. The generated data was stored in .mat files.

6.3 Results for voltage stability assessment using DTs

The set of simulated load data points for the base case network configuration is shown in figure 6.2 with respect to load 5 i.e. for a fixed change in demand at load 6 and load 8, demand at load 5 is changed in small steps. These points were split into a training set (65% of the data) and testing set (35% of the data). The points in the testing set were then classified to regions, based on the classification rules given in chapter 4.

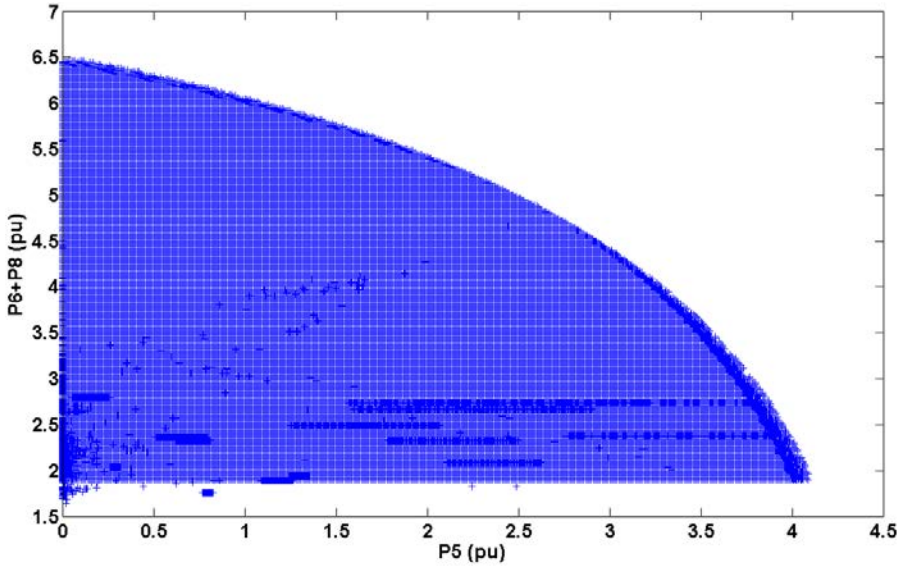

Figure 6.2 Data of different loading conditions for base case with respect to load 5

Figure 6.3 shows the data in figure 6.2 classified as per classification rules.

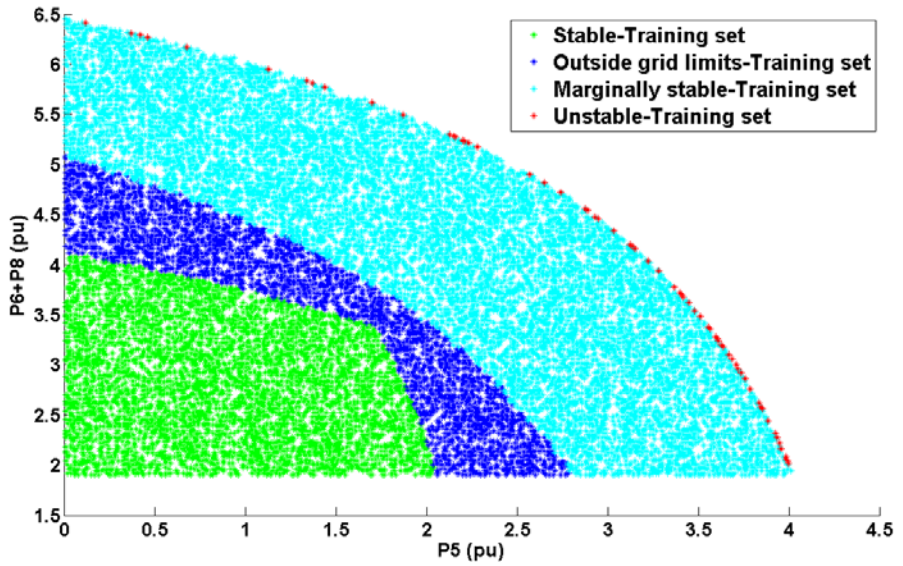

Figure 6.3 Data of different loading conditions for base case with respect to load 5 classified based on classification rules

This classified data was used to create the decision tree for base case network configuration with respect to load 5.

6.3.1 Creating the Voltage Stability Assessment DTs

For a network configuration, decision trees were created for variations with respect to every load. So, every network configuration of IEEE 9 bus system

has three decision trees. The MATLAB function fitctree in Statistics and Machine Learning Toolbox was used to create the decision trees. This function performs the following steps [29].

1. Start with all the input data, and examine all possible binary splits on every predictor.
2. Select a split based best optimization criterion subject to minimum leaf size constraint.
3. Impose the split
4. Repeat steps 1-4 recursively for the two child nodes

The function stops when it cannot make any more splits or if further splits would not improve classification accuracy. The optimal value for minimum leaf size was chosen by calculating the prediction error using the kfoldloss function (Statistics and Machine Learning Toolbox) in MATLAB [29]. This function calculates the error by checking the prediction of the decision trees on trained on particular percentage of training set. For example the training set is divided to two sets with 75% and 25 % data. The decision trees are trained on the 75% of the data and tested on the 25% of data to calculate error. The imposed minimum leaf size versus the cross validated error for base case network configuration is shown in figure 6.4. It can be observed from figure 6.4 that the cross-validated error remains constant for decision tree with respect to load 5 for minimum leaf size greater than 8000. This helps to give insight whether the training set has enough data points to train the decision trees for. It can also be observed from the figure that for decision tree with respect to load 6 and 8 has a constant cross-validated error for minimum leaf size ranging from 3500 to 7500. Based on this cross-validated error the function fitctree sets an optimum value for minimum leaf size when training the DTs. When the leaf size is less than the selected, it stops splitting the nodes.

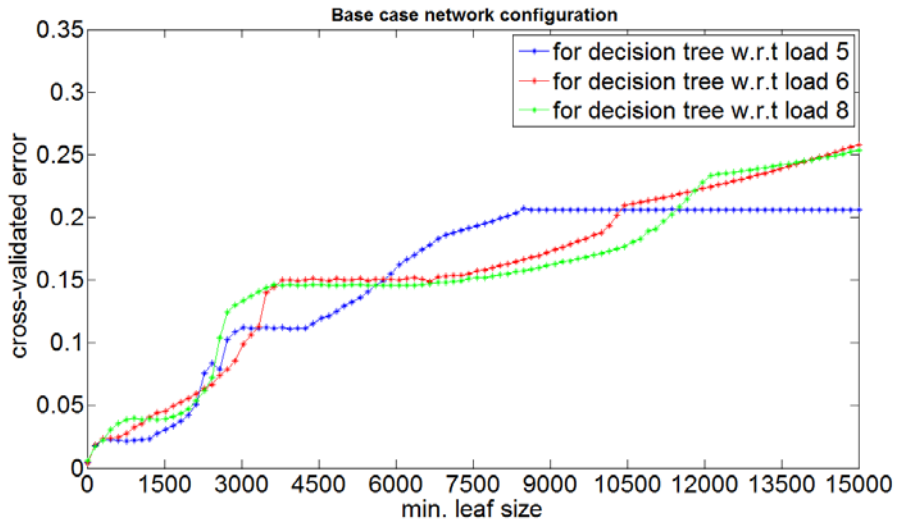

Figure 6.4 Cross-validated errors as a function of min. leaf size for base case network configuration decision trees

The created tree has an average of 35 branches (size). The obtained size is the optimal size based in the cross-validation error as shown in the above figure.

6.3.2 Testing the Voltage Stability Assessment DTs for base case network configuration

The created decision trees for different network configurations were tested on the test set (35% of the data). The test set data was given as input to the created decision trees and these outputs were verified with classification criteria used to create the decision trees. Based on the number of misclassifications by the created decision trees, the accuracy was calculated for base case network configuration with respect to load 5 is tabulated in 6.2.

Table 6.2 Accuracy of the created decision tree with respect to load 5 on test set data for base case network configuration

		Actual:			
Estimated as:	Train/Test 48077/16026	Stable	Out of grid limits	Marginally stable	Unstable
	Stable	100 % (4434/4434)	-	-	-

	Out of grid limits	-	99.96 % (2706/2707)	1	-
	Marginally stable	-	-	99.96 % (8822/8819)	-
	Unstable	-	-	2	99.97 % (64/66)

The values that are given under the percentage in the table are in the format of (estimated/actual). It can be observed from table 6.2 that two operating points in "unstable" region are misclassified as "marginally stable" region and one operating point in "outside grid limits" region is misclassified as "marginally stable". The prediction accuracy is low in "outside grid limits" and "marginally stable" region. The classification accuracy of the decision tree for base case network configuration with respect to load 6 is tabulated in 6.3.

Table 6.3 Accuracy of the created decision tree with respect to load 6 on test set data for base case network configuration

	Actual:				
Estimated as:	Train/Test 41403/13801	Stable	Out of grid limits	Marginally stable	Unstable
	Stable	99.96 % (3037/3036)	-	-	-
	Out of grid limits	1	99.69 % (2592/2600)	7	-
	Marginally stable	-	-	99.88 % (8121/8112)	-
	Unstable	-	-	2	99.96 % (51/53)

It can be observed from table 6.3 that the prediction accuracy is low in "outside grid limits" region since seven operating points are misclassified to "marginally stable" region. The classification accuracy of the decision tree for base case network configuration with respect to load 8 is tabulated in 6.4.

Table 6.4 Accuracy of the created decision tree with respect to load 8 on test set data for base case network configuration

	Actual:				
Estimated as:	Train/Test 47628/15876	Stable	Out of grid limits	Marginally stable	Unstable
	Stable	100 % (3240/3240)	-	-	-
	Out of grid limits	-	99.79 % (3385/3392)	7	-
	Marginally stable	-	-	99.89 % (9191/9181)	-

	Unstable	-	-	3	99.95% (60/63)

It can be observed from table 6.4 that the prediction accuracy is low in "outside grid limits" region since seven operating points are misclassified to "marginally stable" region. It can be observed from table 6.2, 6.3 and 6.4 that even though there are misclassifications, each DT has an average prediction accuracy of 99.9 %.

6.3.3 Testing the Voltage Stability Assessment DTs for outage of line between bus 5 and bus4

The prediction accuracy of decision trees created for network configurations involving outage of the line were tested on test sets and also using time domain simulations results from PSS/E. Time domain simulations were automated by a Python script. The time domain simulations were run for t=20 seconds and the change in network configuration was applied at t=10 seconds.

The details of prediction accuracy on the test set of the created decision tree with respect to load 5 for outage of line between bus 5 and 4 is given in table 6.5. Since the decision trees were created using power flow solutions, it was tested on the time domain simulation outputs from PSS/E. This test was done only for the decision trees that were created for different configuration involving outage of a line.

Table 6.5 Accuracy of the created decision trees for network configuration with outage of line between bus 5 and 4

	Actual:				
Estimated as:	Train/Test 16627/5743	Stable	Out of grid limits	Marginally stable	Unstable
	Stable	99.93 % (1517/1516)	-	-	-
	Out of grid limits	-	99.98 % (250/246)	-	-
	Marginally stable	1	4	99.92 % (3922/3925)	-
	Unstable	-	-	2	96.42 % (54/56)

These decision trees were tested with the output from time domain simulations in the following steps.

1. A set of random load power values were generated.
2. These load powers were applied on the base case network configuration.
3. Time domain simulations were simulated with these load powers on the base case network configuration up to t=10 seconds.
4. At the end of t=10 seconds the change in network configuration was applied and the simulation was continued up to 20 seconds. For example, in this case the time domain simulations were simulated for 20 seconds with line outage between bus 5 and 4 at end of t=10 seconds.
5. Mean load consumptions values and voltages at the load buses from t=18 seconds to end of simulation (t=20 seconds) were considered as input to the trained DTs.
6. Classification criterion was applied on these operating points to verify them with the trained DTs classification.
7. The classification accuracy is calculated and the outputs are plotted to visualize the misclassified operating points by the decision trees.

Classification of time domain simulation outputs using classification criteria and decision tree with respect to load 5 for outage of line between bus 5 and 4 is shown in figure 6.5.

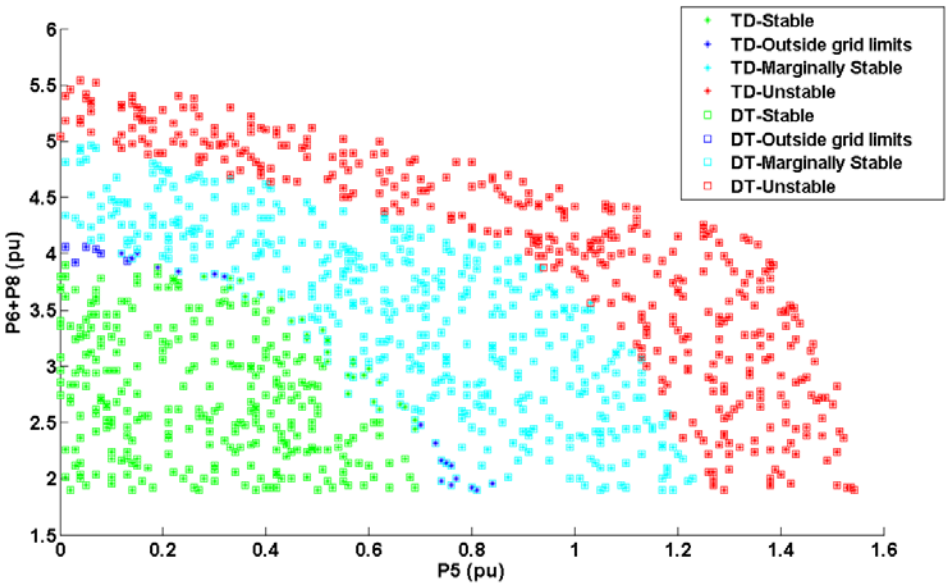

Figure 6.5 Classification of time domain simulation outputs by classification criteria and created decision trees with respect to load 5 for outage of line between bus 5 and 4

It was observed that misclassification happened in the boundary region because of the decimal values of the load powers and voltages (time domain simulations). For example, if 0.25 is the boundary value between two regions ("outside grid limits", "marginally stable"). It was observed that Misclassification happened for the values 0.251, 0.252…0.254 etc. that are classified as "outside grid limits" instead of "marginally stable".

6.4 Results for Pre-calculated Optimal Power Flow Solutions

An Optimal power flow solution was generated for each of the operational points in the training set that do not lie in the "stable" region. The loading margin λ that drives the system to its maximum loading condition is limited to values between 0.1 and 0.25. The lower and upper voltage limits were set to 0.95 and 1.05 pu, respectively. If OPF fails to converge, the optimization problem was relaxed by lowering the minimum voltage limit by 0.01 pu (i.e. if it fails for the first time, the voltage is 0.94 pu) every time it fails to find an OPF solution. Relaxation of the minimum voltage limit is done up to 0.85 pu until OPF finds a solution for the given operating point. If OPF fails to find a solution even after relaxing minimum voltage level to 0.85 pu, then the

voltage limits are completely removed. Even then if OPF still fails to find a solution, then active power direction P_D and reactive power direction Q_D for load reduction is set as shown in the expression in chapter 5. Thus, OPF solutions can be found for all the operating points that do not lie in the "stable" region and are mapped with their corresponding operating point in to database and their outcome when applied to the system.

6.4.1 Generating OPF database

For the given network configuration, OPF solutions were found for the operating points that do not lie in the 'stable' region with respect to every load. For example, for base case network configuration OPF solutions were found for the operating points that do not lie in the 'stable' region with respect to load 5, load 6 and load 8. The OPF solutions to the operating points that do not lie in the 'stable' region for the base case network configuration w.r.t load 5 are shown in figure 6.6.

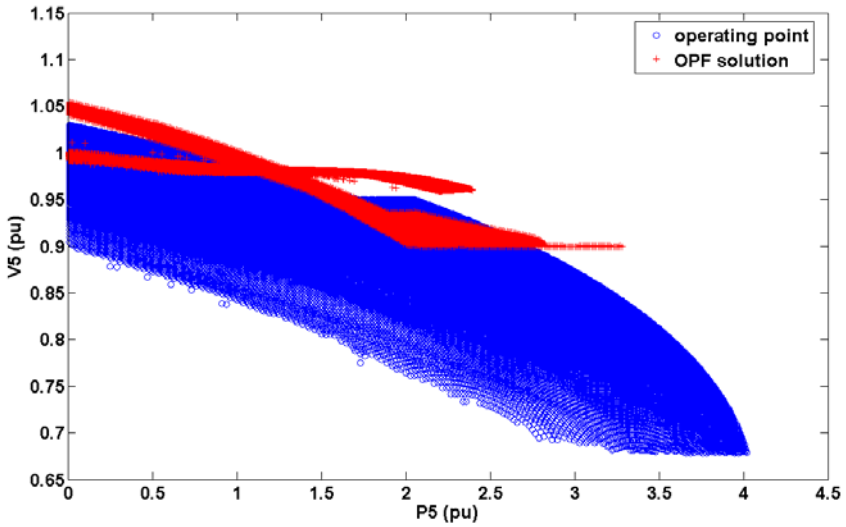

Figure 6.6 OPF solutions of the operating points that do not lie in stable region with respect to load 5

From figure 6.6, all the OPF solutions to the operating points that do not lie in "stable" region lie above the voltage level 0.9 pu. This is because the OPF solution is calculated by imposing the constraints. If OPF solution does not exist for the given constraints, the minimum voltage constraint is relaxed as explained in previous sub-section. So, from the figure it should be noted that

the minimum voltage level is reduced to 0.9 pu. OPF solutions were generated to the operating points (that do not lie in the "stable" region) for different network configuration with respect to load 5, 6 and 8. All these solutions for one network configuration were grouped in to a database and were mapped with their corresponding operating point. This database was used to search for nearest operating point and retrieve its OPF solution.

6.4.2 Testing OPF scheme

The obtained OPF solutions were tested in the following steps.

1. Random load powers were generated using rand function in MATLAB. The function rand returns a vector of uniformly distributed random numbers in the interval (0, 1).
2. These obtained random load values are multiplied with the difference of maximum and minimum load values from the database.
3. Then, these load values were applied to the given network and power flow was simulated.
4. The state of the system was predicted using the decision trees.
5. If the system was not in "stable" region, then the database was searched for the nearest operating point and the OPF solution of the nearest operating point was applied to the system.
6. The state of the system was checked again by DTs after applying the OPF solution.
7. An OPF solution was calculated online for the given operating point and it was compared with the OPF solution retrieved from database.

1000 random load consumption values were created to verify the proposed approach and these load values were applied to IEEE 9 bus system. The number of operating points predicted for each region is given in table 6.6.

Table 6.6 DTs prediction of operating points in different regions

Region predicted by the DTs:	No. of operating points in region:
Stable	303
Outside grid limits	243
Marginally stable	400
Unstable	54

When the OPF solution of the nearest operating points in database was applied to operating points in "outside grid limit" region, some OPF solutions improved the state of the system to "stable" region, while some OPF solutions improved the voltages but not the state of the system. Table 6.7 provides these details for operating points in 'outside grid limits' region.

Table 6.7 No. of operating points that changed state/ remained in same state after applying OPF solution from "outside grid limits" region

Predicted region after applying OPF solution from database	No. of operating points
Stable	62 (25.51%)
Outside grid limits	181 (74.48%)

It should be noted that only 25.51% of the operating points in "outside grid limits" region were improved to "stable" region after applying the OPF solution of the nearest operation point from database. For these 62 operating points, the Euclidean distance to the nearest operational point in the database is shown in figure 6.7. The mean Euclidean distance of these 62 operating points is 0.1256 pu.

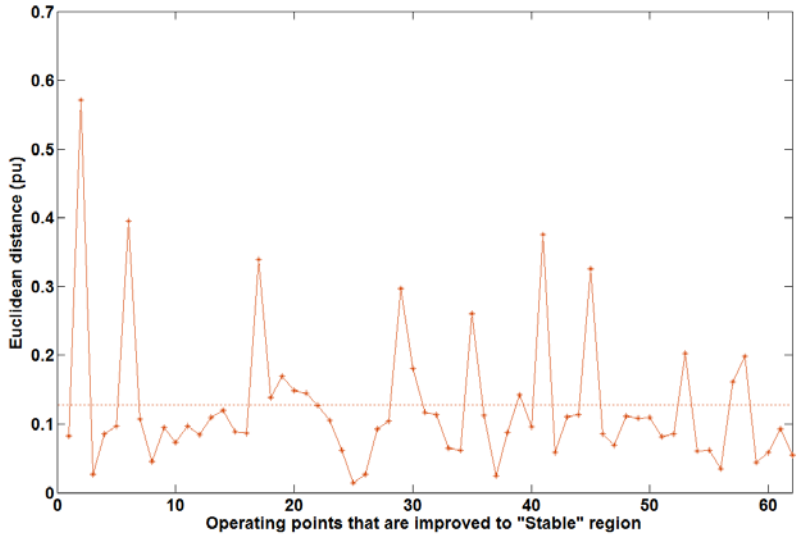

Figure 6.7 Euclidean distance for the improved 62 operating points between the current operating point and the nearest operating point in the database

Figure 6.8 shows the difference in load reduction done for the OPF solution of the nearest operating point from database versus the OPF solution calculated online for the 62 operating points in which system state is improved.

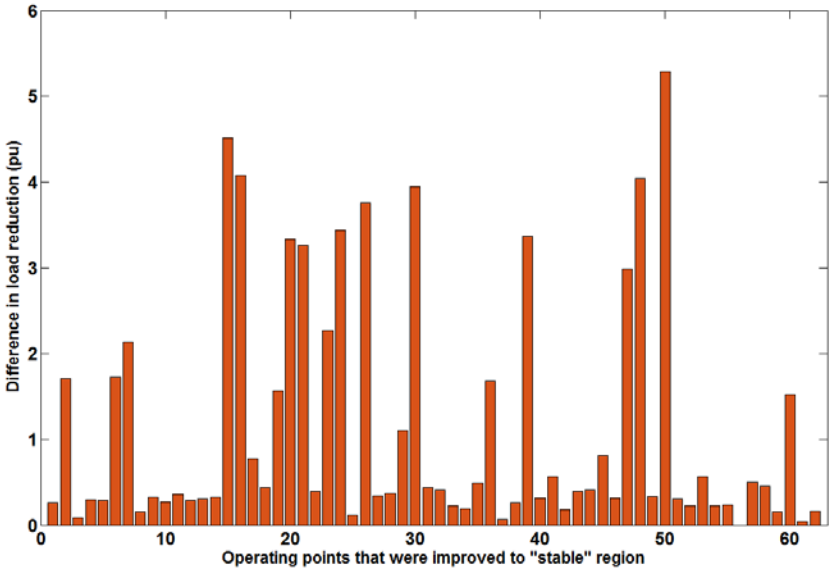

Figure 6.8 Difference in load reductions as per the OPF solution calculated online and OPF solution from database to improve the state from "outside grid limits" to "stable" region

The maximum, minimum and average load reduction required by the OPF solutions for these 62 operating points are given in table 6.8.

Table 6.8 Maximum, minimum and average load reduction by the OPF solution from database and online OPF

	Database (pu)	Online OPF (pu)
Maximum	5.20	2.50
Minimum	0	0
Average	1.15	0.05

Maximum load reduction of 5.20 pu was done only for one operating point and it was located near the boundary of "outside grid limits" region and "marginally stable" region. Out of the 62 operating points, 10 operating points were located in this boundary region for which the load reduction was greater than 3.0 pu. Load reduction in this operating region can be reduced by

having the more operating points with OPF solutions from this region in the database.

When the OPF solution of the nearest operating points in database were applied to operating points in "marginally stable" region, some OPF solutions improved the state of the system to "stable" or "outside grid limits" region, while some OPF solutions improved the voltages but not the state of the system. Table 6.9 provides these details for operating points in "marginally stable" region.

Table 6.9 No. of operating points in each region after applying OPF solution from "marginally stable" region

Predicted region after applying OPF solution from database	No. of operating points
Stable	147 (36.75%)
Outside grid limits	113 (28.25%)
Marginally stable	139 (34.75%)
Unstable	1 (0.25%)

It can be observed from the table that 36.75% of the operating points in "marginally stable" region were improved to "stable" region and 28.25% of the operating points in "marginally stable" region were improved to "outside grid limits" region after applying the OPF solution of the nearest operating point from database. For these 260 operating points, the Euclidean distance to the nearest operational point in the database is shown in figure 6.9.

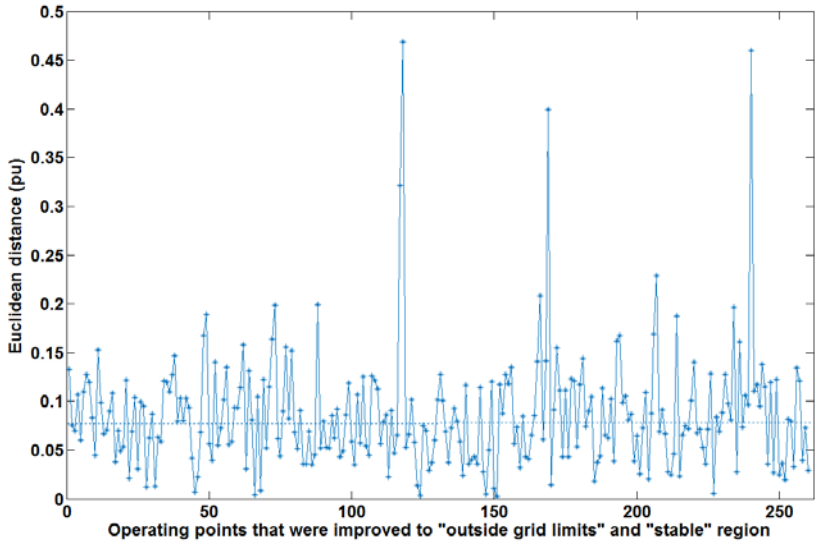

Figure 6.9 Euclidean distance for the improved 260 operating points between the current operating point and the nearest operating point in the database

For these 260 operating points, the mean Euclidean distance to the nearest operating point in database is 0.086 pu. Figure 6.10 shows the difference in load reduction done as per the OPF solution of the nearest operating point from database versus the online OPF solution for the 260 operating points in which system state is improved.

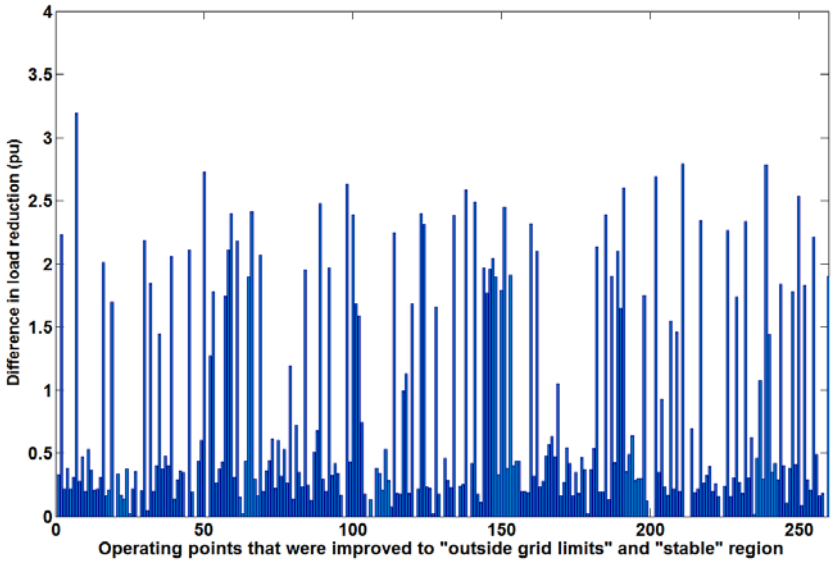

Figure 6.10 Difference in load reductions as per the OPF solution calculated online and OPF solution from database to improve the state from "marginally stable" to "outside grid limits" and "stable" region

The maximum, minimum and average load reduction in these 260 operating cases is given in table 6.10.

Table 6.10 Maximum, minimum and average load reduction by the OPF solution from database and online OPF

	Database (pu)	Online OPF (pu)
Maximum	4.06	5.09
Minimum	0.04	0
Average	1.36	0.65

It should be noted that the maximum load reduction is more for the OPF solution calculated online because the given operating point lies between "marginally stable" and "unstable" regions but the nearest operating point in database is located on the boundary. It was observed from the OPF solutions that the further they are towards "unstable" region, the larger the load reduction in the OPF solution. Since the given operating point is further towards the "unstable" region its exact OPF solution has more load reduction than the OPF solution of the operating point (that is located on the boundary – a bit far from the "unstable" region than the given operating point) from database. This indicates that more operating points are required in the boundary regions to reduce the ambiguity.

It can also be observed that the difference in mean load reduction for improving the state from "marginally stable" region was 0.71 pu and the difference in mean load reduction for improving the state from "outside grid limits" region was 1.1 pu. For one operating point, the system state is deteriorated when applied with OPF solution from database. When it was checked in detail, it was observed that the operating point is misclassified by DTs. The reason for this misclassification is that this operating point is very close to the boundary of "marginally stable" and "unstable" region indicating the significance of the boundary region.

Figure 6.11 shows the percentage of the operating points that are in "stable"/"unstable" region, the operating points for which the OPF solution from database and online calculated OPF solution did not change the region

of operation of the system, OPF solution from database and online calculated OPF solution that improved the state of the system and OPF solution from database and online calculated OPF solution that deteriorated the state of the system respectively.

From figure 6.11, it should be noted that the percentage of operating points for which online calculated OPF solutions improved the state is 3.0 % more than the percentage of operating points for which OPF solutions from database improved the state. Due to misclassification by decision trees there is deterioration of state of operating point (0.1 %) when OPF solution of from database is applied. There are 2.9 % more operating points that remained in the same state after applying the OPF solution of the nearest operating point from database when compared to OPF solution calculated online.

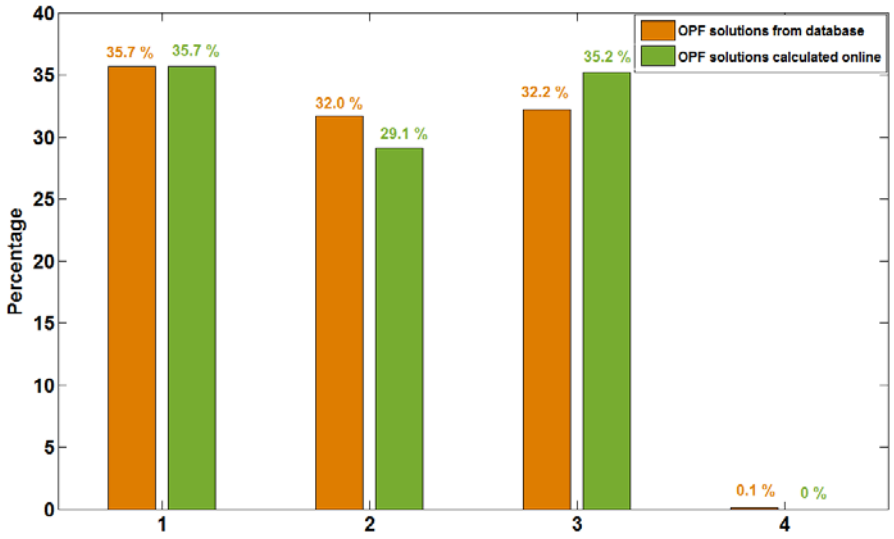

Figure 6.11 Percentage of the (1) operating points that are in "stable"/"unstable" region, (2) the operating points for which the OPF solution from database and online calculated OPF solution did not change the region of operation of the system, (3) OPF solution from database and online calculated OPF solution that improved the state of the system and (4) OPF solution from database and online calculated OPF solution that deteriorated the state of the system

The maximum, minimum and average time taken to search for an OPF solution in database and to calculate OPF solution online is given in table 6.11.

Table 6.11 Maximum, minimum and average time taken to search for an OPF solution in database and to calculate OPF solution online

	Database (sec.)	Online OPF (sec.)
Maximum	1.310	10.12
Minimum	0.211	2.012
Average	0.512	5.561

Table 6.11 shows that the average time taken to retrieve an OPF solution of the nearest operating point from database is 10 times faster than online OPF calculation. Even the maximum time taken to retrieve the OPF solution of the nearest operating point from database is 8 times faster than online OPF calculation. This signifies the advantage of offline computation. It should be noted that the time taken to retrieve OPF solution of nearest operating point and online OPF calculation might vary with respect to the computer configuration that is used for calculations but the mean time taken to search for an OPF solution of the nearest operating point is observed to be less than the time taken to compute OPF solution online. This less time taken to retrieve the OPF solution from database in the proposed approach could be useful to make quick decisions during critical system conditions.

6.5 Advantage of the proposed approach

It took less time to retrieve OPF solution of the nearest operating point from database than to calculate the OPF solution online. This significance was demonstrated by simulating time domain simulation with exponential recovery loads in IEEE 9 bus system with active power time constant set to 5 seconds.

Time domain simulation was run for t=20 seconds with outage of line between bus 5 and 4 is created at t=10 seconds. The operating point was chosen such that the system is heavily loaded. So, when the outage of the line between bus 5 and 4 was created it lead to the instability in the system. It can observed figure 6.12 that system becomes unstable (after the contingency) at the end of simulation. It can also be observed from the figure that after the contingency the load consumption at bus 5 is recovering to the pre-

contingency load power consumption because they are modelled as exponential recovery loads with $\alpha_t = 1$ as in sub-section 5.2.3. As the load power consumption recovers to the pre-contingency load power consumption values, the voltage at the load buses reduces (from equation 5.5, when $\alpha_t = 1$ then $P_t = P^0\left(\frac{V}{V^0}\right)$) as shown in figure 6.12. As the load power consumption recovers, the voltage at the load buses drop leading to oscillations and further making the system unstable. The load bus voltage magnitudes for this contingency are shown in figure 6.13.

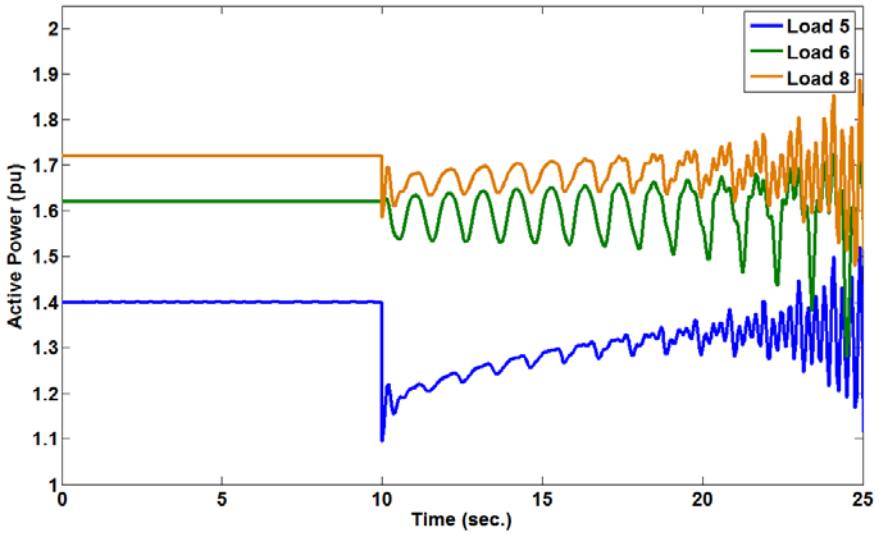

Figure 6.12 Active power consumption at the load buses for outage of line between bus 5 and 4

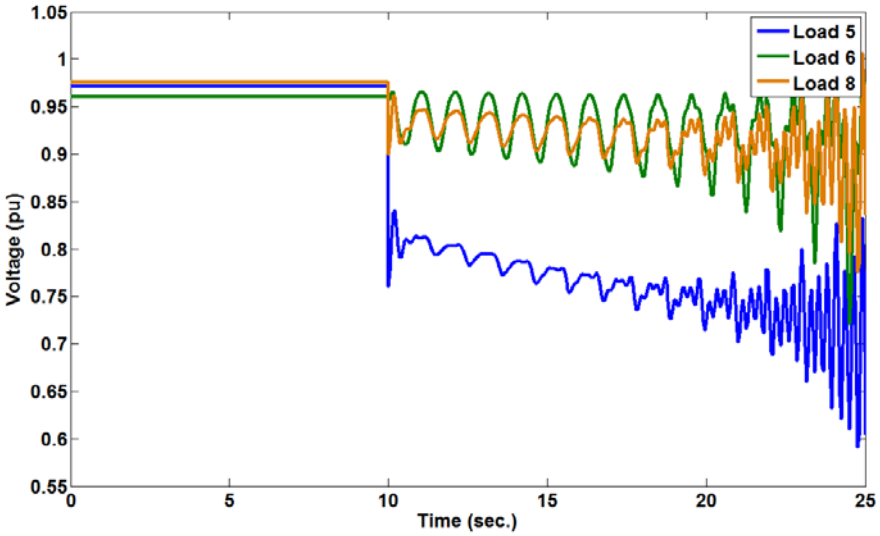

Figure 6.13 Voltage magnitudes at the load buses for a line outage between bus 5 and 4 in IEEE 9 bus system

The proposed approach of using pre-calculated OPF solutions from database is applied to this scenario after 0.512 seconds, i.e. the average time taken to retrieve OPF solution from the database (as shown in Table 6.11). So, the active power and voltage magnitudes at the load buses of the system after applying the OPF solution at 10.512 seconds can be observed in figure 6.14 and 6.15 respectively.

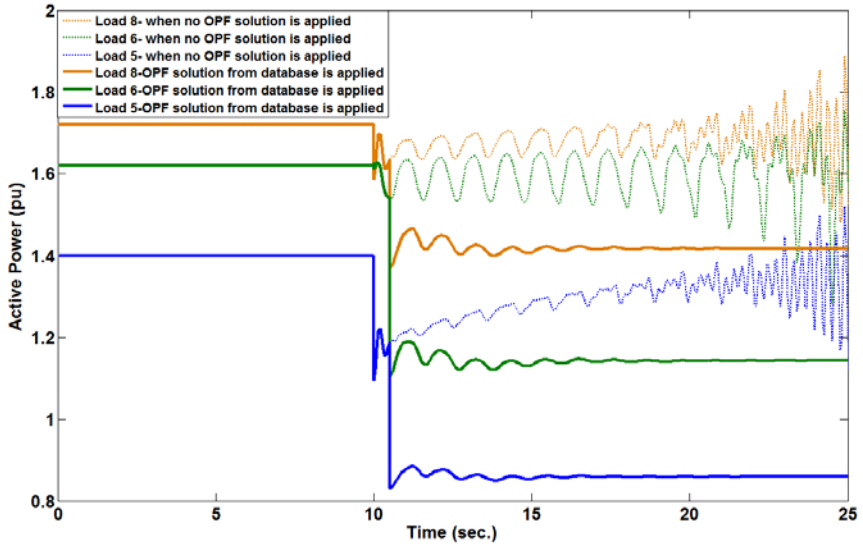

Figure 6.14 Active power consumption for outage of line between bus 5 and 4 after applying the proposed approach

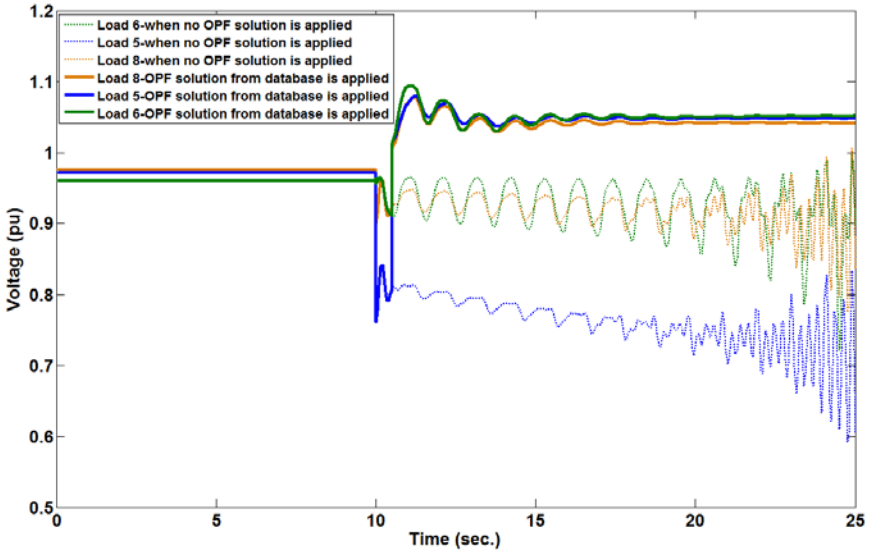

Figure 6.15 Voltage magnitudes at the load buses for outage of line between bus 5 and 4 after applying the proposed approach

The online calculate OPF solution of this operating point is applied to the system 5.561 seconds (from table 6.11) after applying contingency. The active power and voltage magnitudes at the load buses of the system after applying the OPF solution at 15.561 seconds can be observed in figure 6.16 and 6.17 respectively.

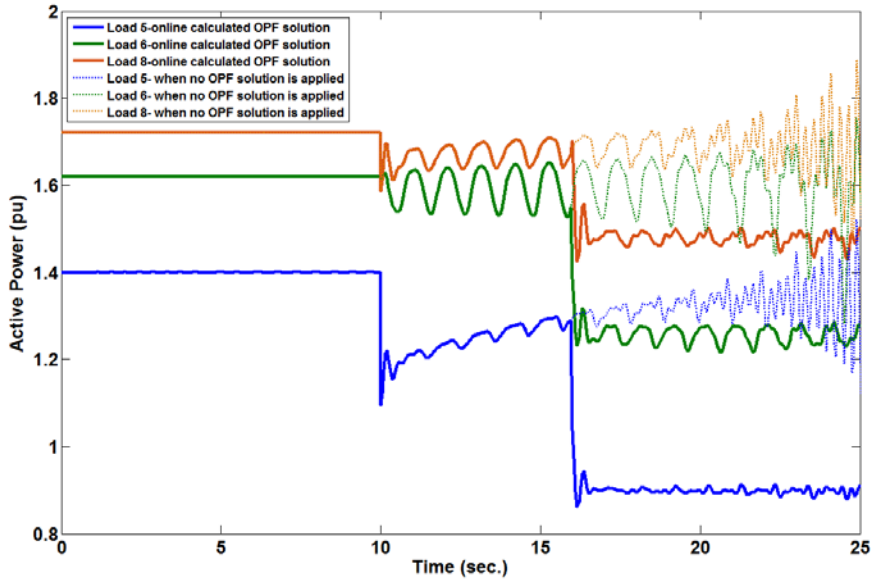

Figure 6.16 Active power consumption for outage of line between bus 5 and 4 after applying the online calculated OPF solution

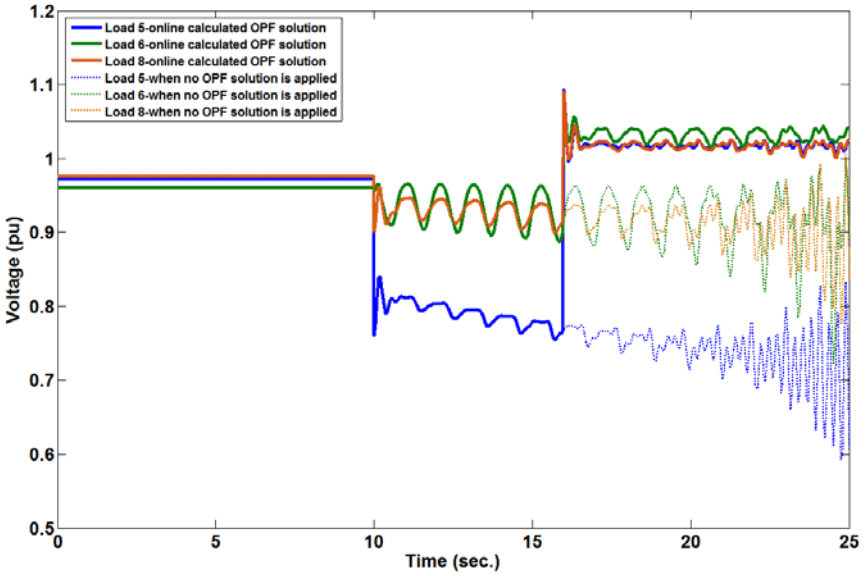

Figure 6.17 Voltage magnitudes at the load buses for outage of line between bus 5 and 4 after applying the online calculated OPF solution

From the figures 6.14 and 6.15, when the OPF solution of the nearest operating point is applied to the system 0.512 seconds (from table 6.11) after the contingency, there is load reduction and improvement in the voltages at the load buses. The oscillations in load consumption and voltage magnitudes are damped after applying OPF solution as shown in figures 6.14 and 6.15.

From the figures 6.16 and 6.17, when the online calculated OPF solution is applied to the system 5.561 seconds (from table 6.11) after the contingency, there is load reduction and improvement in the voltages at the load buses. But the oscillations in load consumption and voltage magnitudes are reduced after applying OPF solution as shown in figures 6.16 and 6.17. It should be noted from figure 6.14 and figure 6.16 that time of application of OPF solution plays an important role in stabilizing the system. Since the proposed method retrieves the OPF solution of the nearest operating point from database in less time than calculating OPF solution online, the system is stabilized when the proposed method is applied as shown in figures 6.14 and 6.15.

6.6 Discussion

The decision trees that are trained on the power flow data to determine the security regions has an average accuracy of 99.96% for IEEE 9 bus system. From the accuracy of the decision tree results on the time domain simulations presented in the sub-section 6.3.3, it was observed that boundary areas of the classified regions are more prone to misclassification. Misclassification can be evaded by including more operational points in the boundary of the classified regions when training the decision trees.

From the results presented in sub-section 6.4.2, (approximately) one third (32.2 %) of the given operating points were improved in the state of the system when OPF solution of the nearest operating point from the database was applied. While other one third (32%) of all the given operating points did not change the system state but the voltages at the load buses were improved.

From the results presented in section 6.5, the time taken to retrieve the OPF solutions of the nearest operating point was considerably less than the time taken to compute the OPF solution online and this approach could be useful to evade the unstable condition by aiding the system operator during critical system conditions.

Chapter 7

7. CLOSURE

7.1 Summary

The growing demand for electricity driven by deregulated electricity markets, has forced modern power systems to operate closer to operating limits. Due to deregulated markets and large scale integration of renewable energy sources the power systems are operating under stress conditions making them vulnerable to a range of contingencies. Because of these reasons, application of new effective security assessment and control methods are essential in evaluating and enhancing the power system's stability. By computing the regions and boundaries for a power system the stability status can be predicted, and, based on these computations, preventive measures can be suggested in order to restore system's stability.

This report has suggested the idea of using decision trees to enlarge and generalize the existing security boundary method of stable and unstable regions to classify the operating regions based on distance from the nearest SNB point. A theoretical background and different steps involved in achieving the objectives (refer chapter-1) were presented and explained in detail in their corresponding chapters.

The workflow used to train the decision trees on the power flow output for different network configurations was presented in chapter-4. Each network configuration has decision trees w.r.t every load bus. These trained decision trees were used to predict the region of operation ("unstable", "outside grid limits", "marginally stable", "unstable") of a power system. The optimization problem from PSAT that is used to calculate the OPF solution of the operating points and the work flow used for calculating OPF solutions was explained and presented in detail in chapter 5.

In the case studies chapter presented in this thesis, the proposed approach was tested on IEEE 9 bus system. Decision trees were created on the training set and tested on the testing set. The accuracy results for the created DTs and the observations on the misclassifications were presented in the sub-section 6.3.2 and 6.3.3. The pre-calculated OPF solutions were mapped to their corresponding operating point to form a database. The proposed approach was tested on random load power values and the advantage of proposed approach was explained with a particular scenario in a power system.

7.2 General Conclusions and Recommendations

The decision trees can be created using the historical data but to get variety of historical data requires long time. Moreover historical data may not contain all type of faults. So, considering these aspects simulated data was used to create the decision trees. The decision trees in this study were created using the power flow results of the given power system model. Therefore, the prediction accuracy of the created decision trees for a real power system depends on the accurate modeling in the power system analysis software.

The decision trees were trained using the power flow results since the time domain simulations take more computational time. The power flow simulations for different network configurations and different load power consumptions were automated in order to reduce total computational time for training DTs.

7.3 Conclusions from Case Studies

The average accuracy of classification by the created decision trees on power flow data for random time domain simulations was 99.06 %. It was observed that the majority of the misclassified operating points lie on the boundary of regions. Therefore, more operating points are required in the boundaries of the regions when training the decision trees in order to reduce the misclassification of operating points in the boundary region.

From the results presented in sub-section 6.4.2, one third of the given operating points were improved in the state of the system when OPF solution

of the nearest operating point from the database was applied. While other one third of all the given operating points did not change the system state but the voltages at the load buses were improved. Due to misclassification by the decision trees, system state was deteriorated when the OPF solution of the nearest operating point from database was applied for one operating point.

It was also shown in the case studies that the time taken to retrieve the OPF solutions of the nearest operating point was considerably less than the time taken to compute the OPF solution online. It should be noted that this could significantly help the operator in scenarios like the one explained section 6.5.

The idea of this approach to use decision trees to classify the operating regions ("unstable", "outside grid limits", "marginally stable", "unstable") based on distance from the nearest SNB point has proved it to be fruitful in applying OPF solution of the nearest operating point in the database because of the less time taken to classify the region and search for nearest operating point OPF solution. However, further study on a bigger power system model is essential to further identify any anomaly behaviors such as impact of voltage control devices like FACT devices, Tap changing transformer or any neglected conditions such as impact of intermittency of the renewable energy generation. Overall, the case studies has shown that the offline computation of the decision trees for different network configuration and pre-calculated OPF solutions can assist power system operators in voltage stability assessment and fast preventive control.

7.4 Future Work

1. The OPF solution of the operating point could possibly be improved by searching for (k) k-nearest operating points within a specified distance and allocate weights (w_i) to the OPF solutions of these operating points (OP). The OPF solution of the current operating point could then be given as shown in (7.1) with respect to (7.2).

$$OPF = \frac{1}{k}\sum_{i=1}^{k} w_i * OPF(OP_i) \tag{7.1}$$

$$s.t. \sum_{i=1}^{k} w_i = 1 \quad (7.2)$$

This could further improve the OPF solution of the operating point.

2. Include the options of how to apply the control actions and their sequence of operation when applying the preventive control on the system based on pre-calculated OPF solution.

3. Use smarter methods to generate the training data e.g. Continuation Power Flow (CPF)

4. In real-world power systems, the loads often depend on both the voltage and frequency at their respective buses. But in this thesis, the load dynamics are neglected by assuming constant PQ loads, which are generally considered as worst case scenario. In order to make the proposed approach to work under realistic power systems scenario, it is essential to model certain percentage of the loads as voltage dependent or frequency dependent loads.

5. The proposed approach should be applied on a larger power system, e.g. IEEE 39-bus system, in order to check if there is any anomalous behavior or short-comings in the proposed approach with the increase in size of the decision trees or computational time etc.

6. The proposed approach should be tested on a system that has voltage controlled buses. Voltage controlled buses maintain constant voltage at a particular bus irrespective of the load consumption at that bus. So, including voltage as an attribute for the creation of decision tree can cause ambiguity problem because the voltage at that bus does not vary as a function of the load consumption at that bus. This could result in erroneous classification of security regions. Proper attribute selection in these cases could be a further research topic.

7. Inclusion of cost for the load shedding to be done as per the OPF solution from the database can help to further develop the existing

method to search for nearest operating point with any possible minimum interruption cost load shedding OPF solution.

8. Using smart methods like Continuation Power Flow (CPF) to generate the training data for decision trees.

BIBLIOGRAPHY

[1] P. Kundur, J. Paserba, V. Ajjarapu, G. Andersson, A. Bose, C. Canizares, N. Hatziargyriou, D. Hill, A. Stankovic, C. Taylor, T. Van Cutsem and V. Vittal, "*Definition and classification of power system stability IEEE/CIGRE joint task force on stability terms and definitions*," IEEE Transactions on Power Systems, vol.19, no. 2, May 2004.

[2] C. A. Cañizares (Editor), *Voltage stability Assessment: Concepts, Practices and Tools*. Tech. Rep., IEEE/PES Power System Stability Subcommittee, Special Publication SP101PSS (ISBN 01780378695), 2003.

[3] C.W. Taylor, *Power System Voltage Stability*. New York: McGraw-Hill, 1994.

[4] P. Kundur, *Power System Stability and Control*. McGraw-Hill, 1994.

[5] T. V. Cutsem, Costas Vournas, *Voltage Stability of Electric Power Systems*. Massachusetts: Kluwer Academic Publishers, 1998.

[6] V. Ajjarapu, *Computational Techniques for Voltage Stability Assessment and Control*. Springer, 2006.

[7] Y. L. Chen, C. W. Chang, and C. C. Liu, *"Efficient methods for identifying weak nodes in electrical power networks,"* IEEE Proceeding-Generation, Transmission and Distribution, vol. 142, no. 3, pp. 317-322, May 1995.

[8] P. S. Bimbra, *Electrical Machines,* Khanna Book Publishers, 2005.

[9] M. A. Pai, *Energy Function analysis for Power System Stability,* Kluwer Academic Publishers, 1989.

[10] IEEE Task Force on Load Representation for Dynamic performance, *Load Representation for Dynamic Performance Analysis,* IEEE Transactions on Power Systems, Volume: 8, Issue: 2, May 1993.

[11] A. G. Phadke, *"Synchronized Phasor Measurements in Power Systems,"* IEEE Computer Applications in Power, vol. 6, pp. 10-15, April 1993.

[12] Jiawei Han, Micheline Kamber, *Data Mining: Concepts and Techniques,* San Francisco: Morgan Kaufman Publishers, 2001.

[13] L. Wehenkel, M. Pavella, *"Advances in decision trees applied to power system security assessment,"* IEE 2nd International conference on Advances in Power System Control, Operation and Management, December 1993.

[14] L. Wehenkel, T. Van Cutsem, M. Pavella, Y. Jacquement, B. Heilbornn, P. Pruvot, *"Machine Learning, Neural Networks and Statistical pattern recognition for voltage security: a comparative study,"* Engineering Intelligent Systems, vol. 2, December 1994.

[15] T. Van Cutsem, L. Wehenkel, M. Pavella, B. Heilbornn, M. Goubin, *"Decision tree approach to voltage security assessment,"* IEEE Proceedings-C, vol. 140, no. 3, May 1993.

[16] J. Carpentier, *"Contribution e lêtude do Dispatching Economique,"* Bull. Soc. Franc. Elect., pp. 432-447, 1962.

[17] Hans Glavitsch, Rainer Bacher, Report on *Optimal power flow algorithms,* Swiss Federal Institute of Technology, Switzerland.

[18] David E. Goldberg, *Genetic algorithms in Search, Optimization and Machine Learning,* Addison Wesley Longman, Inc., 1989.

[19] M. Huneault, and F. D. Galiana, *"A Survey of the Optimal Power Flow Literature,"* IEEE Transactions in Power Systems, vol. 6, no. 2, pp. 762-770, May 1991.
[20] G. L. Torres, and V. H. Quintana, "*Introduction to Interior-Point Methods,"* in IEEE-PICA, Santa Clara, CA, May 1999.
[21] C. A. Cañizares, "*Application of Optimization to Voltage Collapse Analysis,"* in IEEE-PES Summer meeting, San Diego, USA, July 1998.
[22] C. A. Cañizares, W. Rosehart, A. Berizzi, and C. Bovo "*Comparison of Voltage Security Constrained Optimal Power flow Techniques,"* in Proc. 2001 IEEE-PES Summer meeting, Vancouver, BC, Canada, July 2001.
[23] M. Parniani, J. Chow, L. Vanfretti, B. Bhargava and A. Salazar, *"Voltage stability analysis of a multiple-infeed load center using phasor measurement data,"* in Power Systems Conference and Exposition, 2006. PSCE'06. 2006. IEEE PES, 2006, pp.1299-1305.
[24] iTesla project, *iTesla project results (www.itesla-project.eu)*, 2016.
[25] Chengxi Liu, Zakir Hussain Rather, Zhe Chen and Claus Leth Bak, "*An overview of decision tree applied to power systems"*, 2013. International Journal of Smart Grid and Clean Energy.
[26] D. P. Kothari and I. J. Nagrath, *Modern Power System Analysis*, Tata McGraw Hill Publishers, 2003.
[27] Federico Milano, *Power System Analysis Toolbox: Documentation for PSAT version 2.1.8*, January 6, 2013.
[28] D. R. Bigga and M. R. Hesamzadeh, *The Economics of Electricity Markets*, IEEE-Wiley Press, 2014.
[29] The MathWorks, Inc., *Statistics and Machine Learning Toolbox™ User's Guide*, March, 2016.

APPENDIX

IEEE 9-bus System data:

Line Data			
From bus	To bus	R (pu)	X (pu)
4	1	0.0000	0.0576
4	5	0.0100	0.0850
4	6	0.0170	0.0920
7	2	0.0000	0.0625
7	5	0.0320	0.1610
7	8	0.0085	0.0720
9	3	0.0000	0.0586
9	6	0.0390	0.1700
9	8	0.0119	0.1008

Generator parameters	Gen-1	Gen-2	Gen-3
T'_{d0}	8.9600	6.0000	5.8900
T''_{d0}	0.0500	0.0500	0.0500
T'_{q0}	-	0.5350	0.6000
T''_{q0}	0.0500	0.0500	0.0500
Inertia H	9.5500	3.3300	2.3500
Damping D	1.6000	0.6700	0.4700
X_d	0.3615	1.7200	1.6800
X_q	0.2400	1.6600	1.6100
X'_d	0.1508	0.2300	0.2321
X'_q	-	0.3700	0.3200
$X''_d = X''_q$	0.1000	0.2100	0.2100
X_l	0.0600	0.1000	0.1536

IEEET1	
$T_R(sec)$	0.0000
K_A	20.000
$T_A(sec)$	0.2000
V_{RMAX}	3.0000
V_{RMIN}	-3.0000
K_E	1.0000
$T_E(sec)$	0.3140
K_F	0.0630

$T_F(sec)$	0.3500
E_1	2.8000
$SE(E_1)$	0.3034
E_2	3.7300
$SE(E_2)$	1.2884

IEESGO	
T_1	25.000
T_2	0.0000
T_3	1.0000
T_4	1.0000
T_5	12.500
T_6	0.0000
K_1	5.0000
K_2	3.0000
K_3	0.5000
E_1	2.8000
P_{max}	1.0000
P_{min}	0.0000

TRITA TRITA-EE 2016:181
ISSN 1653-5146